State of Tandem Mirror Physics – 1992

G.A. Emmert, G.L. Kulcinski, J.F. Santarius, I.N. Sviatoslavsky

December 1992

FPA-92-11

FUSION POWER ASSOCIATES

2 Professional Drive, Suite 248
Gaithersburg, Maryland 20879
(301) 258-0545

1500 Engineering Drive
Madison, Wisconsin 53706
(608) 263-2308

STATUS OF TANDEM MIRROR RESEARCH
–1992–

G.A. Emmert, G.L. Kulcinski, J.F. Santarius, I.N. Sviatoslavsky

Fusion Power Associates
Suite 280
402 Gammon Place
Madison, WI 53719
USA

December 1992

FPA-92-11

Contents

List of Tables

List of Figures

Chapter 1

Background for the Present Study

1.1 Introduction

When fusion research began in the early 1950's, there were three main concepts pursued around the world [1]: an open confinement configuration called a mirror, a pulsed concept labeled a pinch, and a closed configuration called a stellarator. Over the past 40 years, all of these concepts have undergone considerable modifications and the pinch configuration was essentially dropped in the United States in 1977 [2], the modified version of the mirror dropped in the U.S. in 1986 [3], and the stellarator program essentially suspended in the U.S. in 1991 [4]. Some of these concepts have been continued at a low level in European and Japanese laboratories, but the closed configuration named 'tokamak' now accounts for over 90% of the world's magnetic fusion effort.

The early work on the mirror revealed an attractive reactor configuration that was more amenable to maintenance and repair compared to the closed configurations. By the mid-1980's, there were six major experimental programs and at least ten smaller efforts on the mirror approach (see Fig. 1.1). However, when the United States program ran into financial constraints in the mid 1980's, the USDOE Office of Fusion Energy decided to narrow its development program to one concept, the tokamak [5]. The funding for the tandem mirror (TM) program peaked at 93 \$M/y in 1984 and by 1988 the tandem mirror program was essentially gone in the U.S. (see Fig. 1.2 [6]). At that time, approximately 600 \$M had been spent on the tandem mirror in the U.S. compared to ≈3,000 \$M on toroidal systems (see Figs. 1.3 and 1.4 [7]). Various reasons for the specific choice were given, but the one most often cited is that the physics of the Tokamak is much more advanced than that of the open systems. Continued research into the tokamak configuration, most notably related to ITER [8], as well as the contemporary tokamak power reactor studies embodied in the ARIES [9] project, has revealed serious problems which still need to be addressed before electric utilities will consider such reactors for their power grids. Specifically, divertor operation, disruption control, current drive, and maintenance have proved to be more difficult than originally anticipated. It is worthwhile noting that these problems exist in spite of the fact that the total investment in toroidal magnetic fusion is now approaching 5 \$B in the U.S. (through FY 1993), approximately 7 times that invested in the tandem mirror program (see Fig. 1.4). Worldwide this ratio is more like 20:1 in favor of toroidal systems compared to mirror devices.

The severity of the problems identified in toroidal systems is sufficient to prompt some in the fusion community to reexamine the decision to narrow the world program down to one commercial configuration. In addition, the following legitimate question is now being asked, "*Have recent advances in physics and technology been sufficient to warrant a revival of the mirror program for power or other unique applications (e.g., for a neutron source)*".

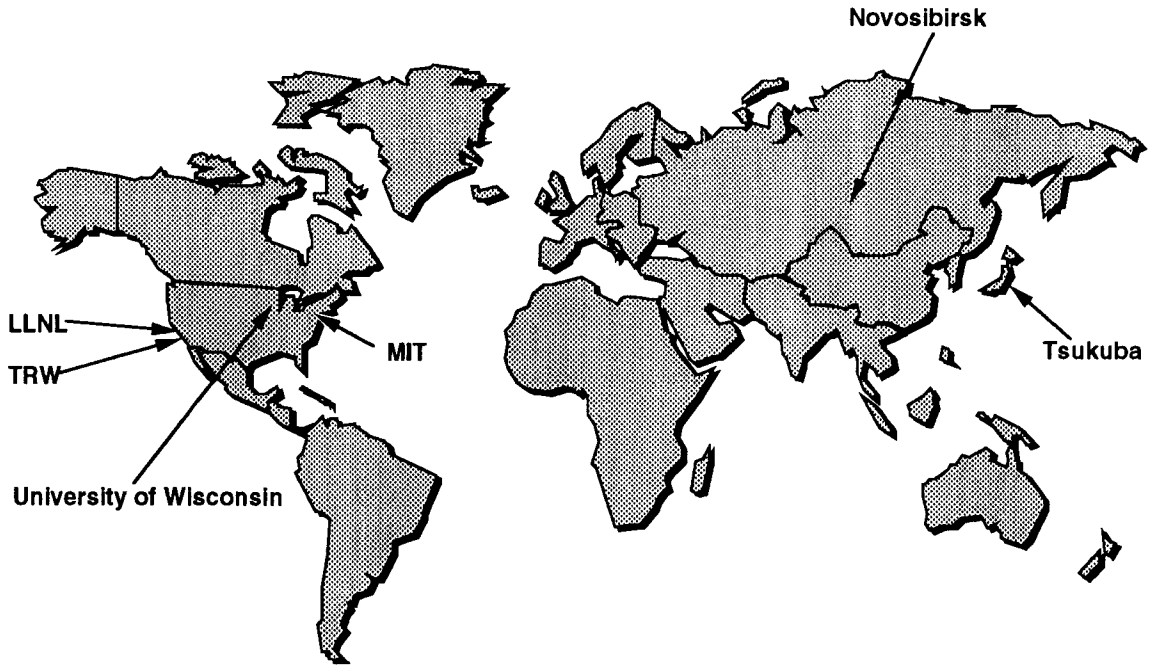

Figure 1.1. *There were six major tandem mirror experimental programs in 1986.*

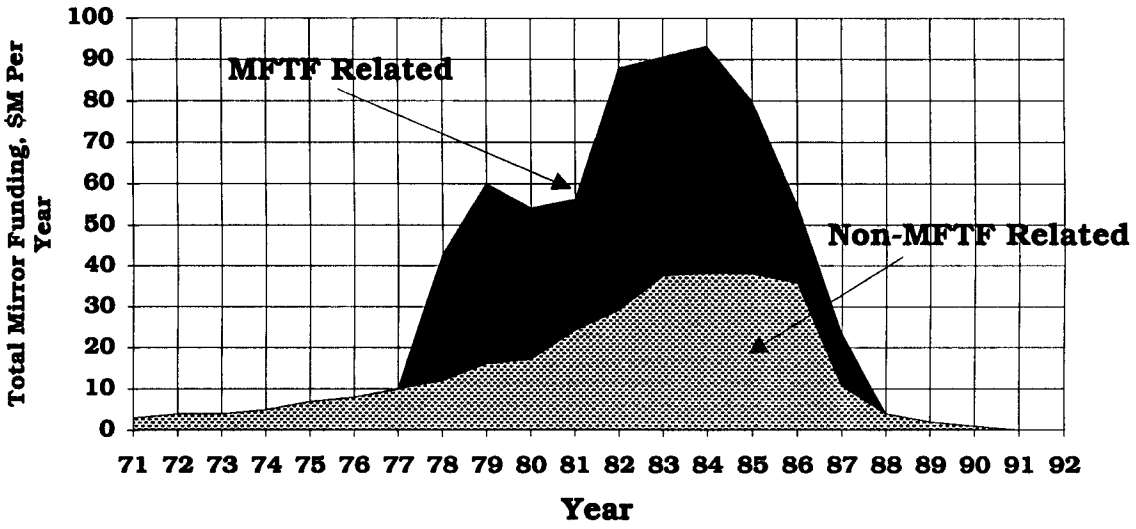

Figure 1.2. *The U.S. tandem mirror program peaked in 1984.*

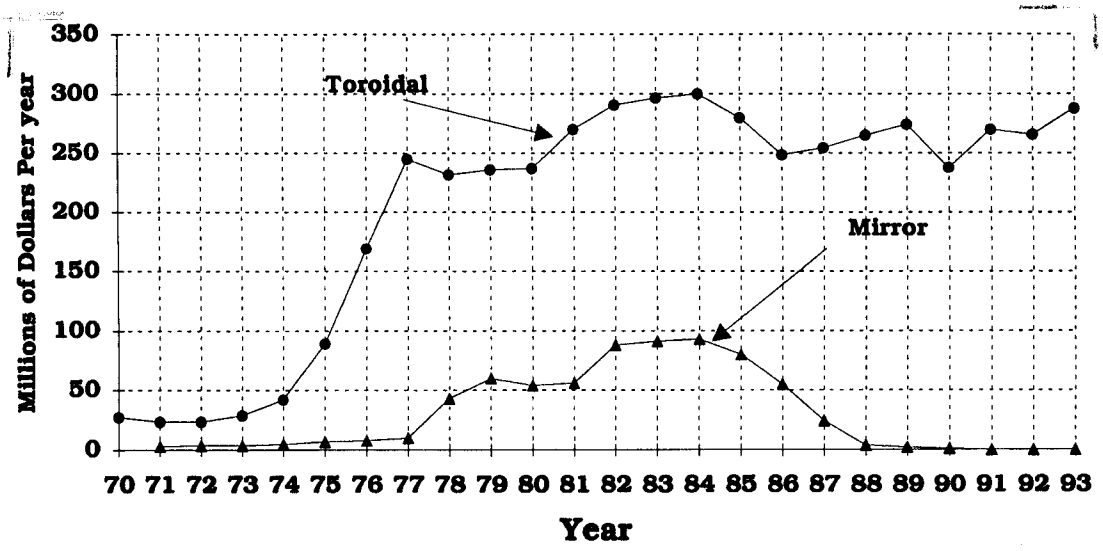

Figure 1.3. *The financial support for the toroidal program in the U.S. far exceeds that for the mirror program.*

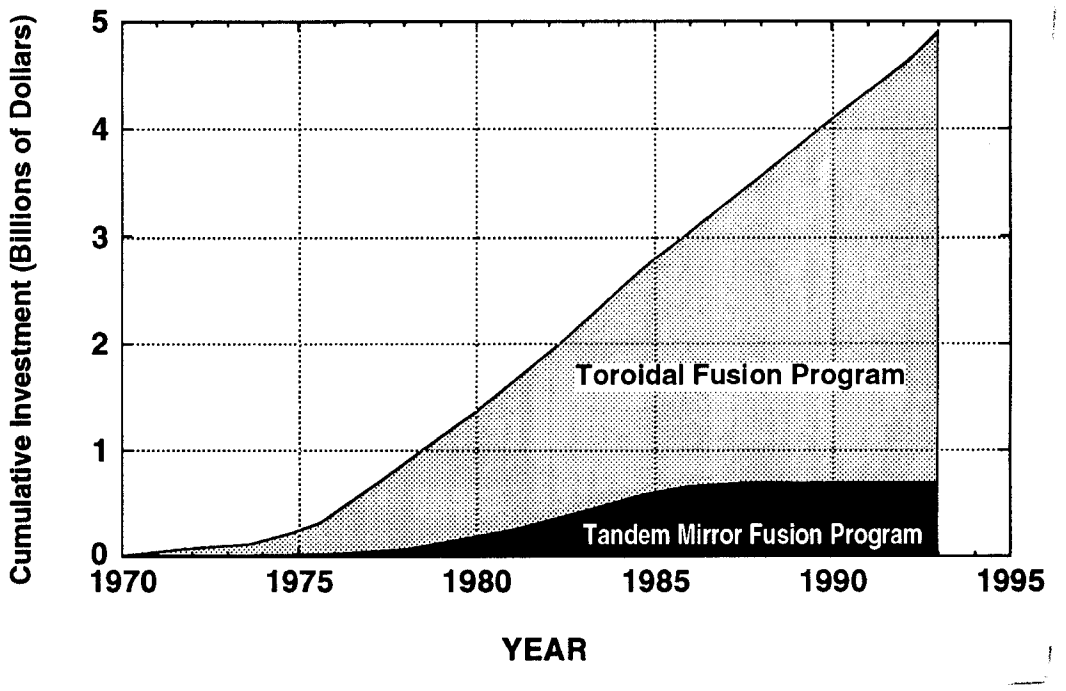

Figure 1.4. *The cumulative investment in the U.S. toroidal fusion program is seven times more than invested in tandem mirror based concepts.*

1.2 Purpose and Organization of This Report

The purpose of this report is to address a few of the key questions on the topic of tandem mirror research and to suggest what, if any, experiments need to be performed to revive the tandem mirror concept for commercial power applications in the 21st century. Because of the limited time allowed for this report ($\approx$3 months), it should not be expected that this study is the ultimate word on these questions. However, it does approach the question of commercial viability from a different perspective and hopefully it will stimulate others in the field to reexamine the future of fusion research.

After a brief review (Chapter 2) of the state of tandem mirror physics at the time of the decision to close the U.S. program, a description of the progress in tandem mirror physics since that decision is given in Chapter 3. Given recent advances in technology and our understanding of power reactor design, Chapter 4 addresses how one might improve the tandem mirror reactor configuration compared to the last full scale design, MINIMARS [10]. The question of critical experiments that could be performed in the 1990's is discussed in Chapter 5 and the overall conclusions plus recommendations are given in Chapter 6.

References for Chapter 1

[1] J. L. Bromberg, "Fusion: Science, Politics, and the Invention of a New Energy Source," MIT Press, Cambridge, MA, 1982.

[2] Ibid., p. 234. See also E.E. Kintner to R.F. Tascek, Dec. 21, 1976 (office files of G.A. Sawyer, LANL).

[3] *Fusion Power Report*, Vol. 7, No. 2, p. 9 Feb. 1986.

[4] *Fusion Power Associates Newsletter*, Dec. 1990.

[5] *Fusion Power Report*, Vol. 7, No. 2, p. 17, March 1986.

[6] The information for this graph came from Dr. A.W. Molvik, LLNL, H.K. Forsen, "Review of the Magnetic Mirror Program," *J. Fusion Energy* 4, 284 (1988), and "Magnetic Fusion Advisory Committee Report on Recommended Fusion Program Priorities and Strategy," DOE/NBM-4004782, Sept. 1983.

[7] Some of the information for this figure came from the National Academy Report, "Pacing the U.S. Magnetic Fusion Program," Nat. Acad. Press, Washington DC, 1989.

[8] "ITER Concept Definition," Vol. 1 and 2, IAEA, Vienna, ITER Documentation Series, No. 3, 1989.

[9] F. Najmabadi, R.W. Conn, et al., "The ARIES-II and ARIES-IV Second Stability Tokamak Reactors," *Fusion Technol.* **21**(3), 1721 (1992).

[10] J.D. Lee, Technical Editor, "MINIMARS Conceptual Design: Final Report," Lawrence Livermore National Laboratory Report, UCID-20773, Vol. I and II, Sept. 1986.

Chapter 2

Status of Tandem Mirror Physics Through 1986

2.1 Introduction

Tandem mirror physics rests on a foundation of thirty years of successful single-cell mirror physics. The combination of simple-mirror cells into the tandem mirror creates some qualitative differences due to the interactions of plasma flowing from one cell to another, but much of the earlier work still applies. Thus, in order to understand the present status of the tandem mirror, the main focus of this report, we will also discuss the parameter achievements and the relevant understanding gained through research on simple mirrors. Several summaries of single-cell and tandem-mirror physics exist [1]–[9], and Ref. [1] has been particularly valuable in comprehensively summarizing progress through 1986.

An attractive fusion reactor must satisfy both *physics* and *engineering* constraints. Historically, toroidal device research was motivated by the physics issue of confinement, whereas mirror machine research was motivated by the engineering issue of beta ($\beta \equiv$ plasma pressure/ magnetic field pressure) [8]. Sufficiently good confinement reduces plasma transport losses so that the required external input power can be minimized. High β allows efficient use of the external magnetic field and minimizes magnet cost. Both confinement and β are critical parameters for fusion reactors. The early toroidal devices exhibited good plasma confinement but they were limited in β, while the early simple mirror devices achieved high β with limited confinement. The characteristic difference in β between reactor geometries remains valid today, but the invention of the tandem mirror has greatly improved the confinement in linear devices. In comparison to toroidal fusion reactors, tandem mirror reactors have several advantages, as listed in Table 2.1.

Historically, as illustrated schematically in Fig. 2.1, mirror devices first solved the magnetohydrodynamic (MHD) stability and microstability problems in *simple* mirrors—which had intrinsically poor confinement due to collisional scattering of particles into the magnetic mirror 'loss-cone.' The invention of the original tandem mirror and the thermal-barrier tandem mirror then eliminated the low theoretical limit on confinement. At present, the key remaining issues for tandem mirrors lie in

- the interactions between plasmas in different cells,
- the RF-plasma interactions,
- the 'pumping' of the electrostatic potential well in the thermal barrier, and
- the generic fusion-reactor issue of the experimentally untested effects of fusion products.

Table 2.1. *Advantages of tandem mirrors over toroidal configurations.*

- The axisymmetric tandem mirror central cells have high β and a magnetic field on the axis that approaches the magnetic field on the coils. This gives high leverage to such designs, because the fusion power density in the plasma scales as $\beta^2 B^4$, where B is the magnetic field.
- No equilibrium plasma current is required, so plasma disruptions do not occur, in contrast to tokamak operation.
- The linear, axisymmetric central-cell geometry greatly simplifies the engineering design in the region of highest radiation fluxes.
- The open-field-line topology is amenable to the direct conversion of charged-particle fusion power to electricity [10, 11], which increases the attractiveness of advanced fuel cycles in tandem mirrors.
- Because most of the transport energy loss is axial, the magnetic flux tube can be expanded to reduce the surface heat flux to more manageable levels than those experienced on divertor plates in toroidal devices.

The history of mirror research is illustrated in Fig. 2.2, where three stages are shown: simple mirrors, original tandem mirrors, and thermal barrier tandem mirrors. Simple-mirror research began in the 1950's [8], and it dominated the first 20 years of the program. The invention of the tandem mirror occurred in 1976 [12, 13], followed by the thermal barrier concept in 1979 [14]. Considerable tandem mirror theoretical understanding had been gained and parameter achievement accomplished before the U.S. Department of Energy mirror research program was terminated in 1986 due to budgetary pressures, but just four thermal-barrier tandem mirrors had been operated, so the concept was only partially developed.

This chapter is organized into various topics in mirror physics, but it is important to recognize that there are strong links between many of these areas. Section 2.2, "Magnetohydrodynamic Equilibrium and Stability," treats the macroscopic stability of the plasma. Section 2.3, "Microstability," deals with the smaller-scale instabilities driven by density, temperature, and velocity-space gradients. Section 2.4, "Transport," discusses the fundamental limits to the loss of particles and energy after instabilities have been eliminated. Electrostatic potentials for tandem mirror thermal barriers and end-plugging are also considered in Sec. 2.4, as is the issue of electron thermal conduction. Fusion-product physics issues are explored in Sec. 2.5. Section 2.6 describes the physics issues that arise during plasma startup. Research on di-

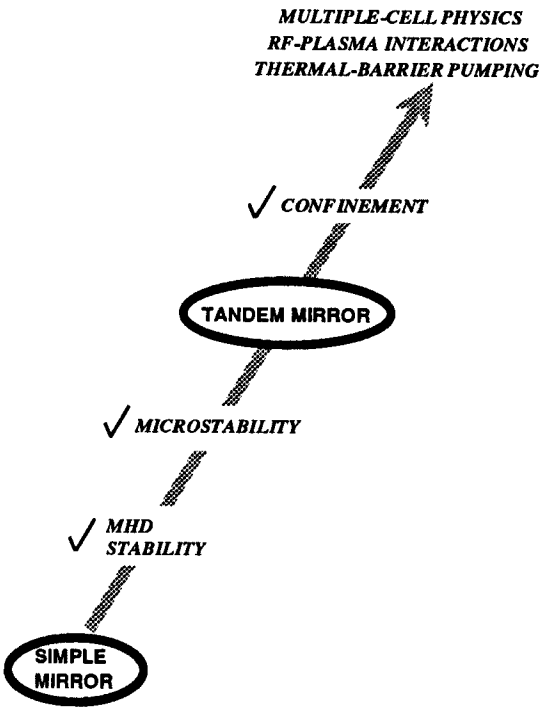

Figure 2.1. *Evolution of mirror configurations.*

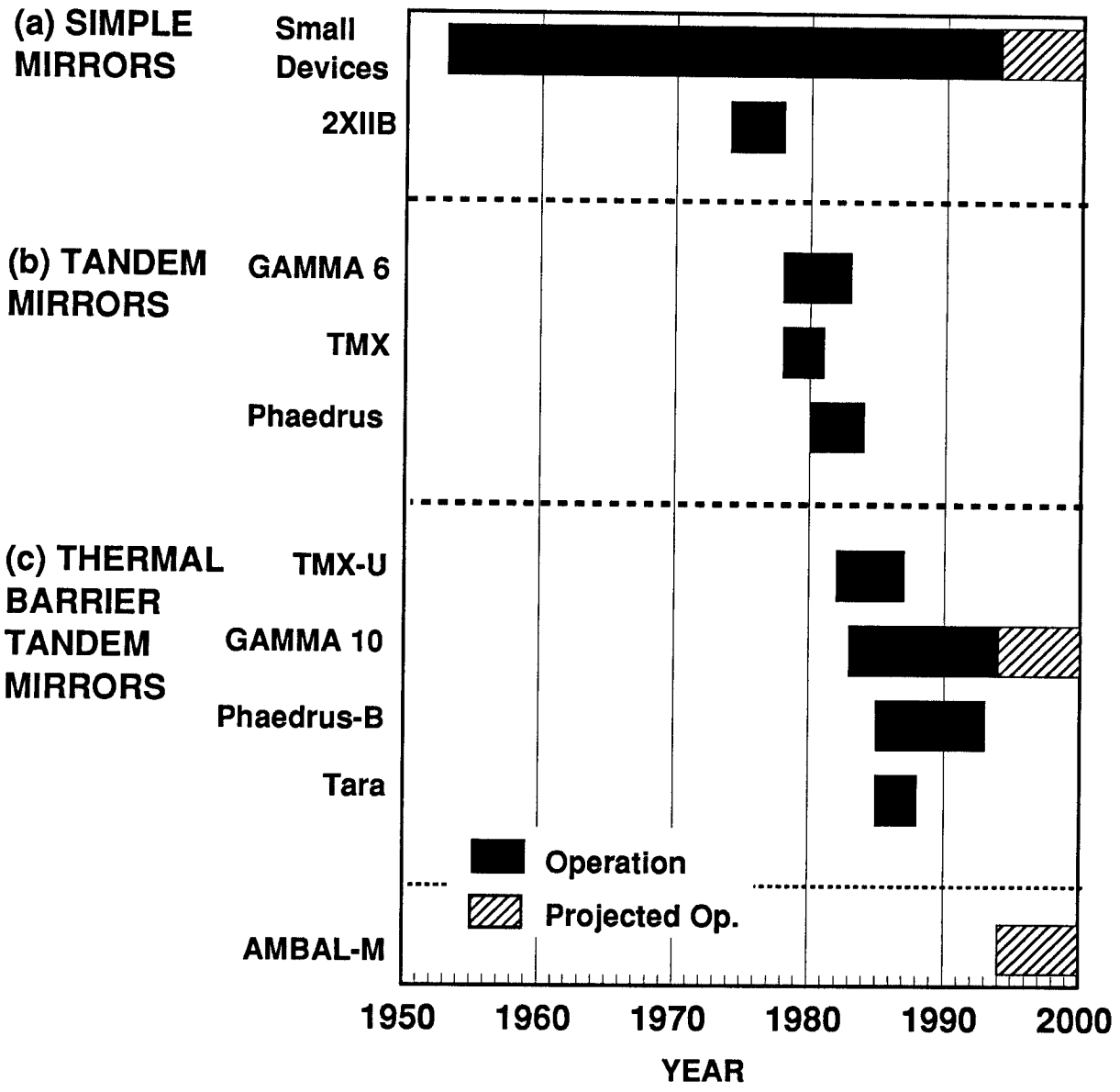

Figure 2.2. *History of the operation of (a) simple mirrors, (b) original tandem mirrors, and (c) thermal barrier tandem mirrors.*

rect conversion of fusion power to electricity is described in Sec. 2.7, and Sec. 2.8 draws some conclusions.

2.2 MHD Equilibrium and Stability

2.2.1 Equilibrium

Generally, a robust magnetohydrodynamic (MHD) equilibrium exists in open-ended devices. This robustness contrasts with the somewhat fragile nature of the equilibrium in a toroidal device, which is sensitive to the closure of the magnetic flux surfaces and to magnetic-field perturbations. The strong mirror equilibrium stems from the externally generated magnetic fields and the existence of adiabatic invariants—which derive from high-frequency motions in comparison to MHD instability frequencies. These invariants, defined in Table 2.2, are the magnetic moment, μ, related to charged-particle gyromotion about the magnetic-field lines; the longitudinal action, J, related to the bounce motion of charged particles between the magnetic mirrors; and a flux invariant, Φ, related to the azimuthal drift motion of the plasma. The adiabatic invariants are of fundamental importance in maintaining the equilibrium, because losses from the non-Maxwellian ion population can be limited

- to the relatively slow process of pitch-angle scattering (changing μ) due to collisions or nonadiabatic effects, and
- to the normally even slower process of radial transport (changing J) due to drift motions resonant with the ion or electron bounce frequencies (ω_{bi} and ω_{be}).

The adiabatic invariants are well understood and experimentally verified [1]. In fact, investigations into the magnetic moment in mirror machines generated important contributions to chaos theory [15]. Finite-β mirror equilibria for arbitrary geometry can be calculated with high accuracy [16].

Table 2.2. *Mirror machine adiabatic invariants.*

INVARIANT	DEFINITION
μ	$mv_\perp^2/2B$
J	$\oint v_\parallel \, ds$
Φ	$2\pi \int B(r)\, r \, dr$

2.2.2 Minimum-B MHD Stability

The macroscopic (MHD) stability of mirror devices can be extremely good, because open-field-line geometry allows the formation of absolute minimum-B magnetic wells (exemplified by the 'baseball' coil in Fig. 2.3). The plasma in a minimum-B equilibrium effectively sees a 'magnetic hill' on all sides, which suppresses low-frequency MHD instabilities ($\omega \ll \omega_{ci}$, where ω_{ci} is the ion-cyclotron frequency). A key consequence of minimum-B geometry is that $\bar{\beta} \to 1$ can be achieved, as experimentally demonstrated in 2XIIB at high average plasma density and temperature ($\bar{n} \simeq 2 \times 10^{20}$ m^{-3}, $\bar{E}_i \simeq$ 13 keV) [17]. Much of the high-β capability of simple mirrors carries over into tandem mirrors, where an appropriate average over stable and unstable cells must be done. In performing such averages, modes which localize in unstable cells must be avoided, such as the trapped-particle mode [18] (see Sec. 2.2.4). In the TMX tandem mirror, where 'yin-yang' magnets created minimum-B end cells, volume-averaged beta values of 40% were reached in a short, neutral-beam-heated section of the central cell [19]. The predictive capability for the MHD equilibrium and stability of both simple mirrors and minimum-B stabilized tandem mirrors is excellent [1]. This reflects both the extensive early effort on simple mirrors and the fact that mirror

geometry is relatively simple to model theoretically.

2.2.3 Axisymmetric MHD Stability

Important developments in achieving high-β, axisymmetric tandem mirror operation emerged in the mid-1980's. These were the possibilities of RF stabilization, wall stabilization, magnetic divertor stabilization, sloshing-ion stabilization, and non-paraxial design.

The Phaedrus tandem mirror experiment first demonstrated the use of *RF stabilization* to maintain MHD stability with both the end cells and the central cell axisymmetric, and central cell beta values exceeding 15% were achieved, even in this relatively small experiment [20, 21]. Figure 2.4 shows the dramatic reduction of density fluctuations for an RF-stabilized case (a) compared to an unstable case (b) in the Phaedrus experiment [20]. The RF-stabilization problem generated a very active research effort, and theoretical models matched well with experimental results [22, 23].

Wall stabilization would theoretically allow very high β (~80–90%) with no injected power, although external power would be required for

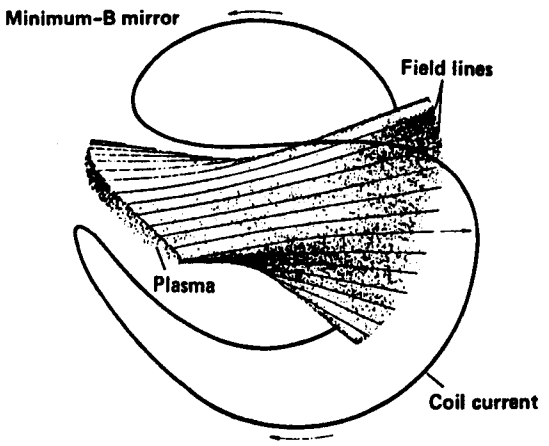

Figure 2.3. *Minimum-B magnetic-field geometry in a 'baseball' coil [1].*

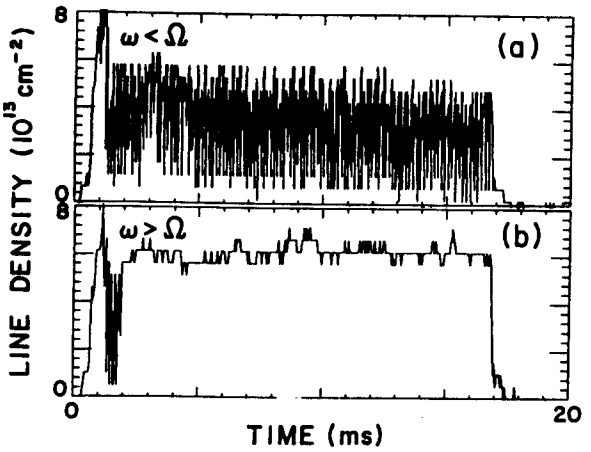

Figure 2.4. *Density fluctuations for (a) unstable case and (b) RF-stabilized case in the Phaedrus experiment [20].*

real systems and during startup at lower β values [24]. The concept is well-grounded in the same MHD theory that predicts other tandem mirror and tokamak stability boundaries with good accuracy. Wall stabilization may have been observed in a small, multiple-mirror device [25].

The use of a *magnetic divertor* in the central cell was also proposed to help provide MHD stability [26]. The proposed divertor would also be axisymmetric, and its stabilizing effect would be to allow good electron mobility in the annular flux tube near the magnetic x-point, thereby 'shorting out' growing instabilities.

The possibility that the *sloshing-ion* neutral beams in the plug could produce an ion distribution with sufficient pressure in the good magnetic-field curvature region to give MHD stability has been proposed theoretically, but has had no experimental test [27, 28].

Similarly, theoretical work indicates that *non-paraxial* mirror cells, defined as cells whose radius is comparable to their length, may allow axisymmetric MHD stability [28]. The implications of the large volume of the non-paraxial mirror cells on the design of a tandem mirror reactor have not been analyzed, especially with

regard to their impact on the power balance requirements.

2.2.4 Trapped-Particle Modes

In the early 1980's, concern arose that electrostatic modes localized to regions of 'bad' magnetic-field curvature might exist [18]. A key objective of the Tara experiment [29] was to test this *trapped-particle* mode theory in its 'axicell' tandem mirror configuration. The axicell concept [30] was developed in order to avoid some of the difficulties related to the use of minimum-B end cells (see Sec. 2.4.6). For axicell configurations, the thermal barrier and end-plugging potential are formed in an axisymmetric cell between the central cell and a minimum-B cell (anchor) that provides the MHD stability. The relative isolation of the MHD anchor cells makes the configuration particularly susceptible to these modes.

2.2.5 MHD Summary

Simple-mirror MHD equilibrium and stability are very well understood. Experiments have achieved $\beta \rightarrow 1$ at high density and temperature, and theory provides an excellent predictive capability at all β values. The understanding of minimum-B stabilized tandem mirrors is almost as good at modest β ($\lesssim 25\%$), but higher β values could not be tested experimentally because of device design limitations. Axisymmetric tandem mirror operation has achieved $\beta \lesssim 15\%$, limited by design power, while theoretical limits on axisymmetric tandem mirror operation approach $\beta = 1$. The 'trapped-particle' mode appears to be important only in 'axicell' configurations. Experimentally achieved and theoretically predicted β values are shown in Fig. 2.5.

2.3 Microstability

2.3.1 Overview

Simple mirrors and the end cells that reduce plasma loss from tandem mirror central cells unavoidably contain non-equilibrium (non-Maxwellian) plasma populations. Therefore, the free energy of the non-Maxwellian populations can be tapped to drive so-called *micro-instabilities*, which appear primarily in two forms:

1. Velocity-space instabilities, caused by a population inversion due to the depletion of low-energy particles that is intrinsic to simple-mirror confinement, and
2. Spatial gradient instabilities, usually caused by anisotropy in pressure, but also by variations in density or temperature alone.

Another useful distinction is between *electrostatic* modes, which are driven by charge separation and can persist to $\beta \sim 0$, and *electromagnetic* modes, which involve perturbed cur-

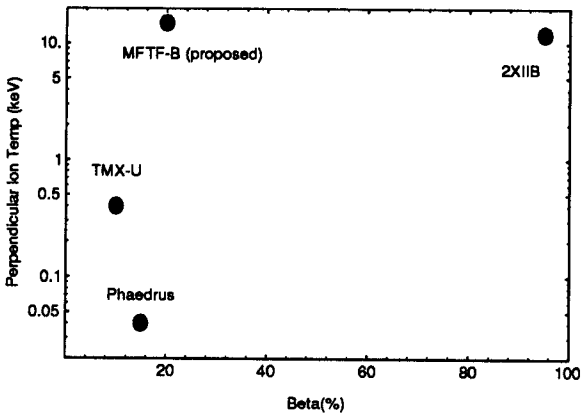

Figure 2.5. *Beta-value operating space for mirrors and tandem mirrors.*

rents and magnetic fields, necessitating finite β. Unlike MHD instabilities, which can cause an immediate movement of the bulk of the plasma into the device walls, microinstabilities cause a relaxation of the plasma distribution function toward an equilibrium state—usually, but not always, strongly enhancing particle diffusion and loss thereby.

The earliest mirror experiments were plagued by several microinstabilities caused by very narrow ion energy distributions, because little collisional broadening occurs at low densities [4, 1]. The successful theoretical effort to understand these experiments set the stage for stabilizing the high-density modes of fusion-relevant plasma regimes. High density is defined by the condition $\omega_{pi}^2 \gg \omega_{ci}^2$, with $\omega_{pe}^2 \simeq \omega_{ce}^2$, where ω_{pi}, ω_{ci}, ω_{pe}, and ω_{ce} are the ion and electron plasma and cyclotron frequencies, respectively. In this regime, electron mobilities force the ion-driven modes to be flute-like ($k_{||} \ll k_{\perp}$), and the modes are qualitatively different from those in low-density conditions [1]. Sufficiently pathological distributions can drive many instability modes, as illustrated in Fig. 2.6, which shows how various combinations of plasma waves and dissipative mechanisms give rise to the indicated instabilities [4]. However, only a few modes are important for realistic distribution functions in the high density and temperature plasmas of the reactor regime.

2.3.2 DCLC and AIC Modes

In the reactor regime, the two most dangerous instabilities are the drift cyclotron loss cone (DCLC) mode and the Alfvén ion cyclotron (AIC) mode. A triumph of the mirror research program was the stabilization of the DCLC mode in the TMX tandem mirror experiment and the subsequent stabilization of both the DCLC and the AIC modes in TMX-U. The result was that extremely low fluctuation levels could be achieved in the TMX-U experiment [31]. The stabilization of the DCLC mode is brought about by partially filling the loss cone in the ion distribution function with a small amount of warm plasma. In TMX, DCLC stability was accomplished using the end-loss ion stream. In TMX-U, warm plasma was trapped in an electrostatic potential well formed in the end plug by 'sloshing ions'—an ion distribution peaked away from the plug midplane and generated either by perpendicular, off-midplane injection or by angled injection at the midplane. The amount of warm plasma in the loss cone required to stabilize the DCLC mode also effectively stabilizes instabilities that had been important in 2XIIB and other simple-mirror experiments: the high-frequency convective loss-cone (HFCLC) mode and the absolute loss-cone (ALC) mode [1].

The only important *electromagnetic* instability in the reactor regime is the AIC mode, and TMX-U was designed to be stable to it through the injection of angled end-plug neutral beams to give a sloshing-ion distribution with a sufficiently high ratio of parallel to perpendicular plasma pressure, $P_{||}/P_{\perp}$. The enhanced microstability more than compensates for the slight increase in diffusive, collisional losses, which occurs for a sloshing-ion distribution because the average ion is located nearer to the loss boundary.

2.3.3 Microstability Summary

An excellent understanding of microinstabilities in mirrors and tandem mirrors has been achieved, including a great deal of confidence that they can be avoided in the design of future experiments and reactors [1]. Because even minimum-B mirror geometry is relatively simple to model theoretically, even nonlinear mirror theory is well understood in comparison to modelling of toroidal geometry (especially with a rotational transform). A prime example is the DCLC mode in 2XIIB, where the instability normally reached nonlinear saturation at fluctuation levels below those of the AIC mode—in

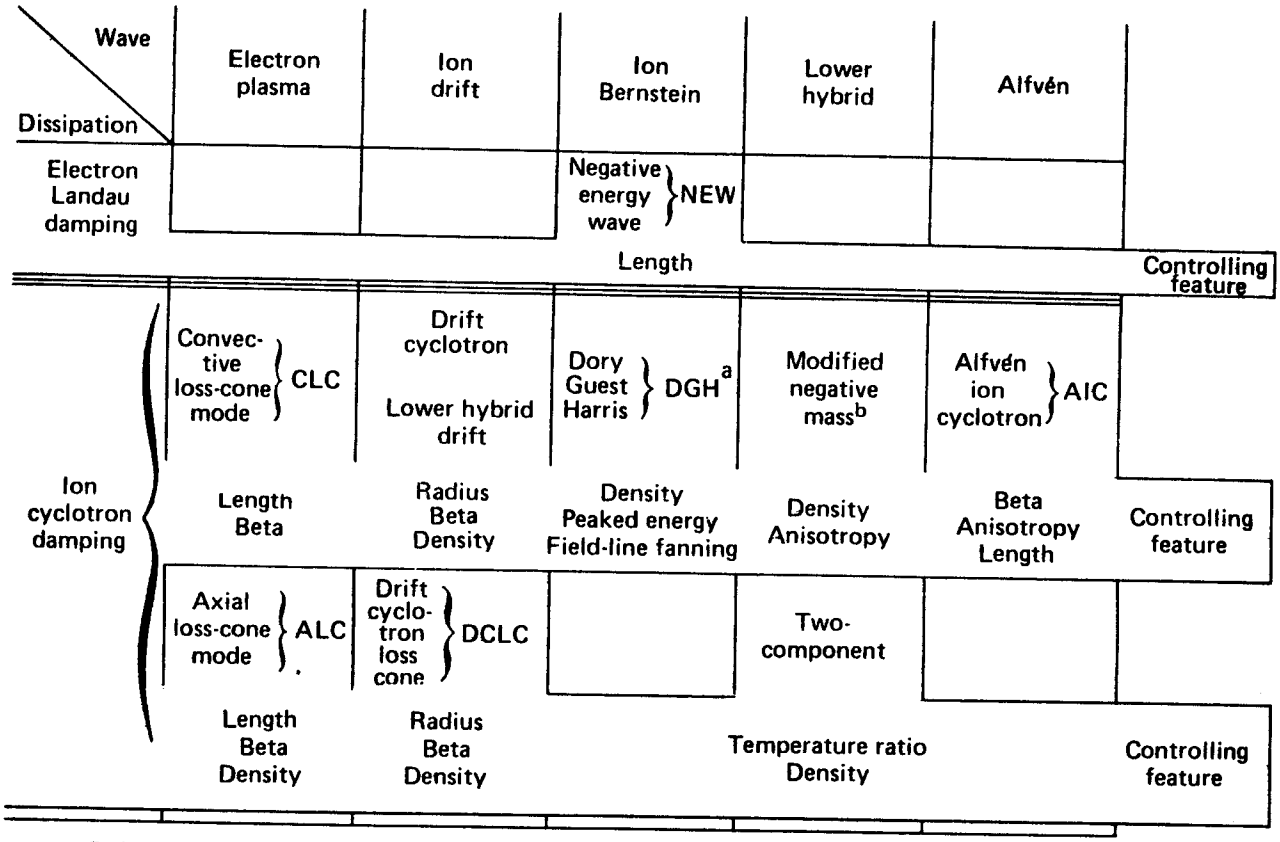

a Strictly speaking, this mode was not destabilized by cyclotron damping, but did arise from the negative-energy nature of the medium.

b Here the anisotropy was the drive, but the mode also required the inclusion of the ion-bounce motion.

Figure 2.6. *Microinstabilities driven by various combinations of plasma waves and dissipative mechanisms [4].*

contrast to the expectations from linear theory. A quasilinear analysis of the filling of the ion distribution's loss cone by warm plasma generated by the DCLC mode itself quantitatively explained the instability boundaries [32].

Regarding the status of microstability knowledge in mirrors and tandem mirrors, Post [1] gives a succinct summary:

> *While continued care must be exercised in future devices, it can be concluded that achieving adequate control of microinstability modes should be possible in mirror systems, in agreement with the predictions of theory. This conclusion represents a major milestone in mirror research.*

2.4 Transport

2.4.1 Overview

In 'collisionless' mirror devices, particle and energy losses stem primarily from ion and electron diffusion in velocity space and subsequent loss along the open magnetic field lines. The term 'collisionless' in this context implies that the collisional mean free path is longer than the length of the device, so that a particle traverses the device many times before experiencing a significant change in its pitch angle with respect to the magnetic field. For most practical purposes, mirror plasmas of interest for fusion are collisionless.

Because the pitch-angle scattering of electrons is $(m_i/m_e)^{1/2}$ faster than that of ions, electrons scatter into the loss cone more quickly than ions, and an ambipolar electrostatic potential forms to reduce electron losses and enhance ion losses so that their loss rates are equalized. The structure of the electrostatic potential along the axis of a simple mirror machine is shown in Fig. 2.7. The physics of the electrostatic potentials and the calculation of the related loss of particles and energy will be discussed in Sec. 2.4.5.

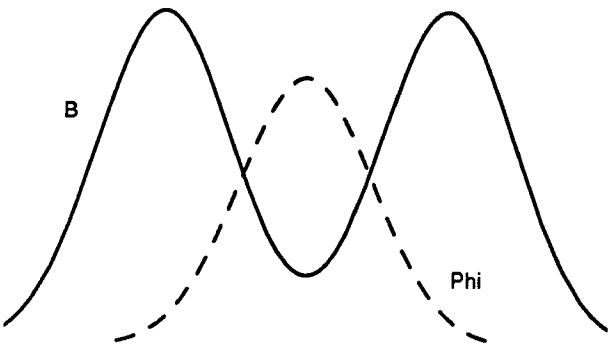

Figure 2.7. *Simple-mirror electrostatic potential profile along the axis.*

2.4.2 Electron Thermal Conduction

An early issue for mirror machines was whether energy loss due to electron thermal conduction along open field lines to the walls could be kept small. In devices where the electron mean free path exceeded the axial length—such as Baseball II, 2XIIB, and the tandem mirror experiments—energy losses were many orders of magnitude below the losses that would have occurred if classical electron thermal conduction dominated. This thermal insulation from the walls occurs because the main electron energy loss mechanism, rather than collisional electron energy transfer, is the escape of relatively few electrons over an electrostatic potential hill.

The basic physics of classical thermal conduction applies, of course, to both mirror and toroidal devices. The key difference between them lies in the way that particles and energy are lost. In mirrors, the loss of particles that have diffused into the mirror loss cone is essentially instantaneous, so that the plasma density in the velocity-space loss cones and, therefore, beyond the magnetic mirror peaks, is a very small fraction of that in the main plasma. Thus, no effective medium for thermal conduction exists. In tokamaks, diffusion takes place in configuration space, with preferential ion loss due to large banana orbits, so that the ambipolar potential acts to reduce ion loss and enhance electron loss. No loss cone exists for most tokamak particles, so the scrape-off layer is relatively dense, and electron thermal conduction can be an important effect.

2.4.3 Electrostatic Potentials

The high mobility of Maxwellian electrons along magnetic field lines leads to a Maxwell-Boltzmann distribution function and, consequently, to an electrostatic potential that depends logarithmically on the density:

$$e\Phi(s) - e\Phi_0 = T_e \ln \frac{n(s)}{n_0} \qquad (2.1)$$

where T_e is the electron temperature $\Phi(s)$ and $n(s)$ are the potential and density along a magnetic field line, and Φ_0 and n_0 are their values at a reference point—typically the midplane. Because a small number of high-energy electrons are lost over the electron-confining ambipolar potential, the distribution is not exactly Maxwell-Boltzmann, but the difference is negligible for most purposes.

When the ion density is locally increased or decreased, for example by neutral beam injection or radial transport, the electron density adjusts to give the appropriate electrostatic potential profile. Figure 2.8 illustrates the axial variation of magnetic field, electrostatic potential, and densities in the GAMMA-10 experiment. This

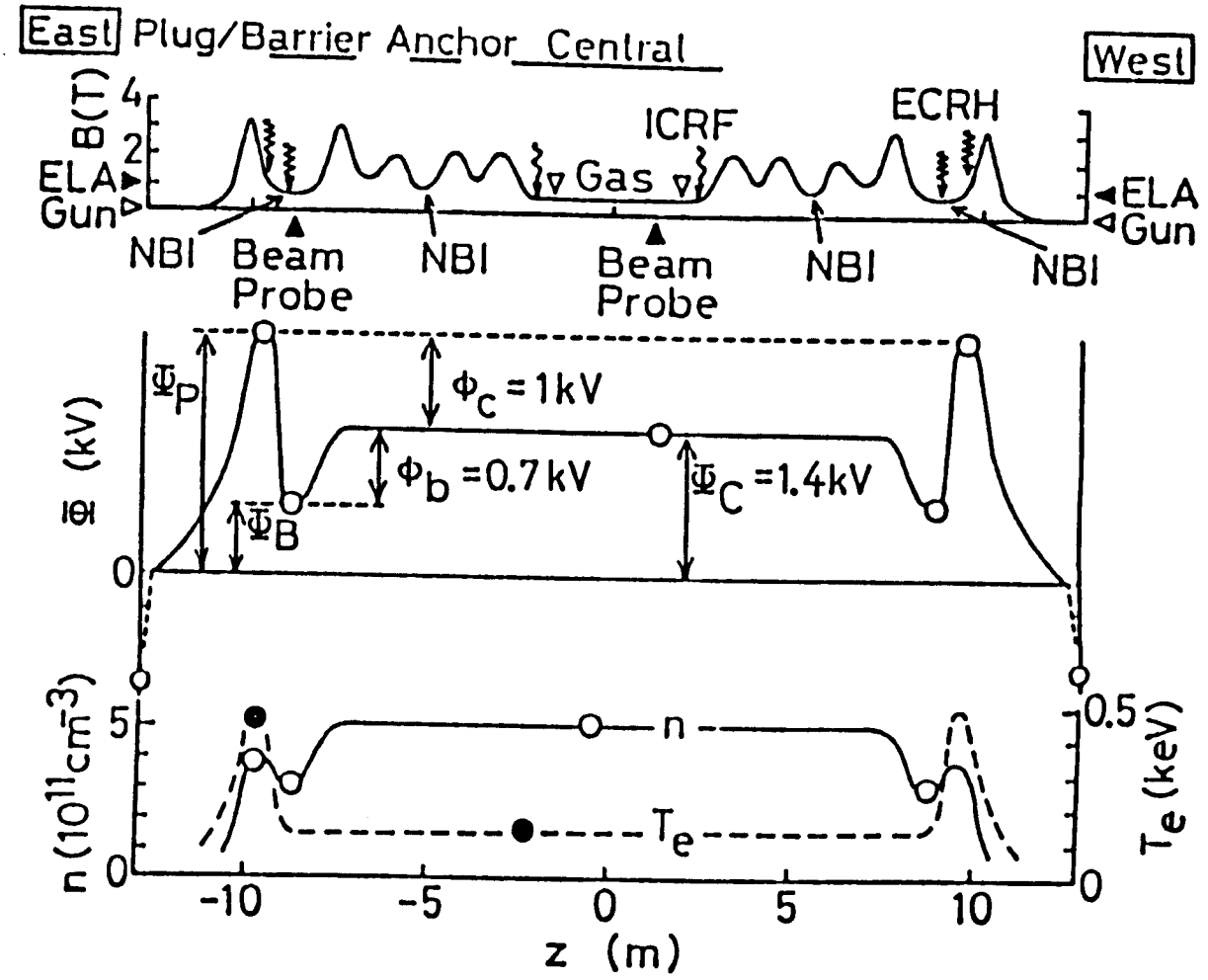

Figure 2.8. *Axial profiles of magnetic field, electrostatic potential, and densities in the GAMMA-10 experiment [33].*

ure shows both the the ion-plugging potential (see Sec. 2.4.5) and the electrostatic thermal barrier (see Sec. 2.4.4). Tandem mirror electrostatic potentials are experimentally verified and reasonably well understood [1].

2.4.4 Thermal Barrier Physics

The creation of a thermal barrier potential is usually more complicated than indicated by Eq. 2.1. The thermal barrier potential dip is initially created by the reduction of the magnetic field, with a consequent expansion of the magnetic flux tube and reduction of the ion density. However, such a potential well will quickly fill up due to ion-ion scattering if no active ion pumping is done. Such pumping will never be perfectly efficient, so an analysis of the pumping process must be included in the calculation of the potential. Furthermore, a non-Maxwellian, hot-electron population localized at the bottom of the thermal barrier is often used to further reduce the density of Maxwellian, passing electrons. The appropriate formula for the electrostatic potential in the thermal barrier then becomes

$$e\Phi(s) - e\Phi_0 = T_e \ln \frac{n_{ec}(s)}{n_i(s) - n_{eh}(s)} \qquad (2.2)$$

where, at position s, $n_{ec}(s)$ is the density of central cell electrons (which pass through the thermal barrier region and return after reflecting off of the ambipolar potential, Φ_e); $n_i(s)$ is the barrier ion density; and $n_{eh}(s)$ is the density of 'hot', mirror-confined electrons—which are generated with a high ratio of perpendicular to parallel energy using electron cyclotron range of frequencies heating (ECRF). Tandem mirrors can operate without the hot electron population, but the resulting ECRF power requirements are high, and most tandem mirror reactor designs invoke hot electrons [34, 35, 36].

Thermal barrier research has focused on three key problems: (1) the thermal barrier filling rate due to collisions, (2) methods for pumping trapped ions out of the thermal barrier, and (3) details of the thermal barrier electrostatic potential axial and radial profiles.

Thermal barrier collisional filling Several theoretical treatments have been performed which treat the problem of the rate at which ions collisionally scatter into the thermal barrier region and partially 'fill' the electrostatic potential well [37]–[41]. Although the calculational methods are quite different, the results for the barrier filling rate agree reasonably well. An experimental test of the barrier filling rate has been performed on GAMMA-10 [33], where the numerical coefficient, the density, and the ion parallel temperature dependence of the lifetime of the unpumped thermal barrier agreed well with the Futch-LoDestro formula [37].

The radial and axial variations of the plasma and magnetic field parameters along a magnetic flux tube are generally neglected in the theories, and the assumption of square-well axial dependence is used. In real devices, the magnetic field and electrostatic potential profiles will be qualitatively similar to those in Fig. 2.9, raising the question of the importance of the regions far from the square-well reference point at the barrier midplane.

Thermal barrier pumping The initial paper on the thermal barrier concept [14] suggested several barrier-pumping possibilities, and neutral beams emerged as the leading candidate in the early experimental and conceptual reactor design work. The TMX-U experiment successfully demonstrated thermal barrier pumping by neutral beams [43], but the WITAMIR-I reactor study showed that the engineering constraints of injecting the beams at the proper angles and of minimizing the injected power make neutral-beam barrier pump-

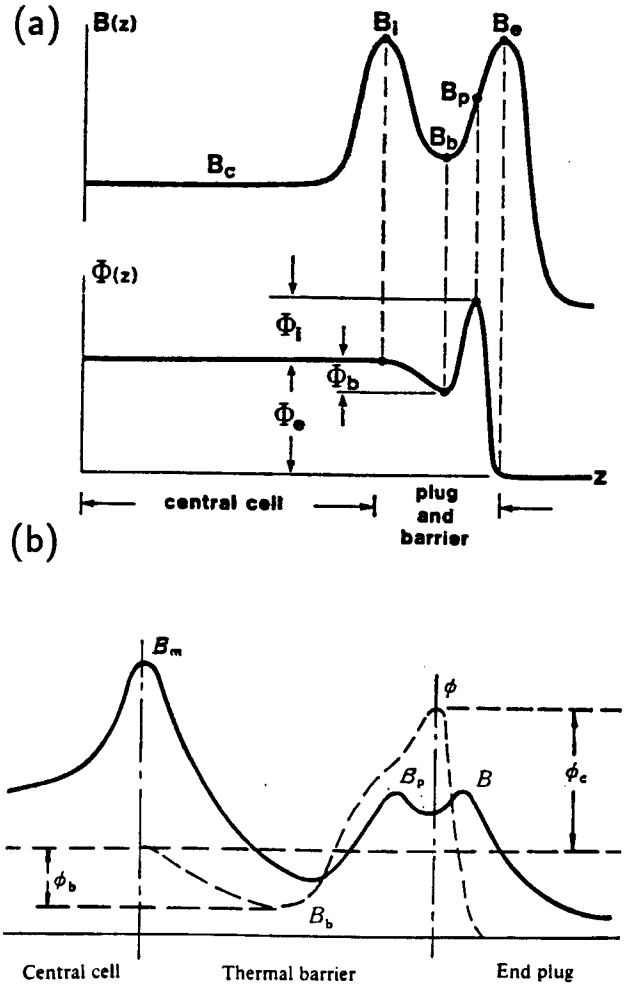

Figure 2.9. *Typical magnetic field and electrostatic potential profiles in thermal barrier tandem mirrors: (a) barrier and plug in the same cell [42] and (b) barrier in a separate cell [40].*

ing very difficult [34]. Therefore, the idea of *drift pumping* by radio frequency waves that generate a perturbed, perpendicular magnetic field, $\tilde{B}_\perp$, began to dominate [44, 45] and it was used for the MARS reactor design [35]. Unfortunately, subsequent calculations indicated that the plasma response to the RF waves reduces the effectiveness of $\tilde{B}_\perp$ drift pumping predicted by the initial theories. Thus, motivated by experiments that showed plasma losses could be induced by the RF ponderomotive force [46], the idea of using the ponderomotive force to pump the thermal barrier through $\mathbf{E}_\theta \times \mathbf{B}$ drifts was proposed [47]. The MINIMARS conceptual reactor design used a variant of this idea to pump the barrier through the enhanced diffusion caused a time-varying RF field and ponderomotive force [36]. As discussed in Sec. 3.4.4, RF-produced thermal barriers were subsequently produced experimentally.

Thermal barrier electrostatic potential The basic theory of the electrostatic potential in thermal barriers is straightforward, but its measurement is difficult. Fortunately, the techniques of heavy-ion beam injection and Langmuir probes provide fairly good data, and the existence of thermal barriers has been well verified experimentally [43, 31, 33, 48]. The initial results from the TMX-U experiment appear in Fig. 2.10.

Another issue is the calculation of the thermal contact between the 'passing' central cell electrons and the 'warm' trapped electrons in the end plugs. The theoretical problem is difficult and is only tractable with simplifications [49, 42]. Although the experimental results generally validate the theory, they are sufficiently inconclusive to motivate alternative theories [31].

2.4.5 Axial Loss

An elegant theoretical analysis exists for the axial particle and energy losses of species confined by electrostatic potentials in mirror machines and tandem mirrors. This analysis was originated by Pastukhov [50] for electrons, was extended and generalized by Cohen and coworkers [51], and was subsequently further refined [52, 53]. The trapped and untrapped regions of velocity space for this problem are shown in Fig. 2.11. The magnitude of the losses is hard to calibrate experimentally. However, the theoretically predicted dependence of the loss on $\exp(\Phi/T)$ has been verified over a wide range of parameters, as shown in Fig. 2.12 [54].

Tandem mirror end cells necessarily contain 'hot', magnetic-mirror-confined ions, and often 'hot' electrons as well. The energy of the hot species is generally high enough so that particles collisionally scattered into the relevant magnetic mirror loss cones are not contained by the electrostatic potentials and are immediately lost out the ends of the machine. The most accurate method of calculating losses for these species is through the use of Fokker-Planck computer codes, which are available, but a relatively simple model for neutral-beam-injected hot ions that contains the most important physics effects—the collisional pitch-angle scattering and the electron drag—has also been developed [55]. The strong interaction of hot electrons with the ECRF that generates them has precluded the development of an analogous model, although some simple estimates have been used for parametric studies [36].

The central cell in a reactor will produce high-energy fusion products: 3.5-MeV alpha particles in D-T reactors or 3.7-MeV alphas and 14.7-MeV protons in D-^{3}He reactors. If the axial magnetic field gradient at the central cell ends is too high, the fusion products can be *nonadiabatic*. That is, they can experience a resonance between their bounce motion and gyromotion that causes large changes in the adiabatic invariant μ. The result of these large $\Delta\mu$'s is that the affected fusion products quickly scatter into the mirror loss cones and escape over electrostatic potentials that are much smaller than the ion's parallel energy. To maintain adiabaticity

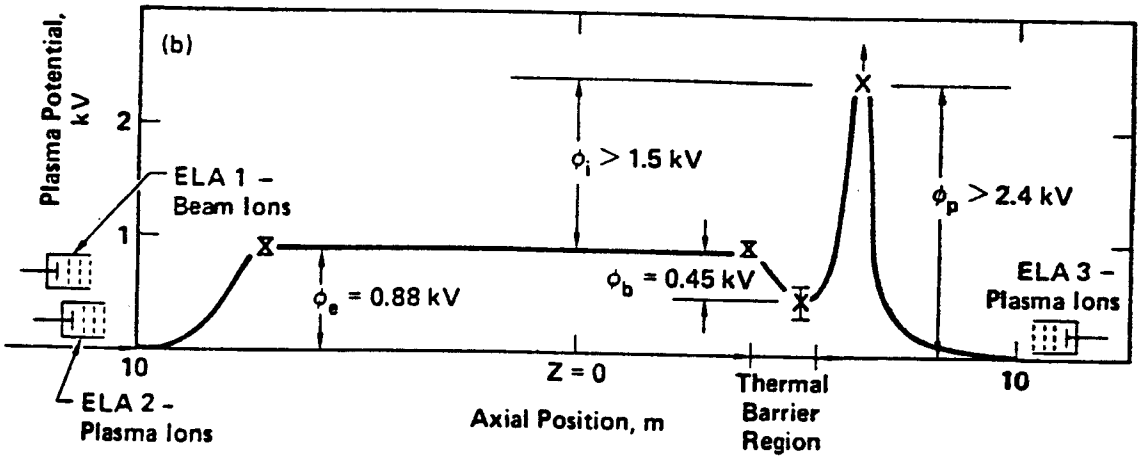

Figure 2.10. *Initial thermal barrier measurements in TMX-U [43].*

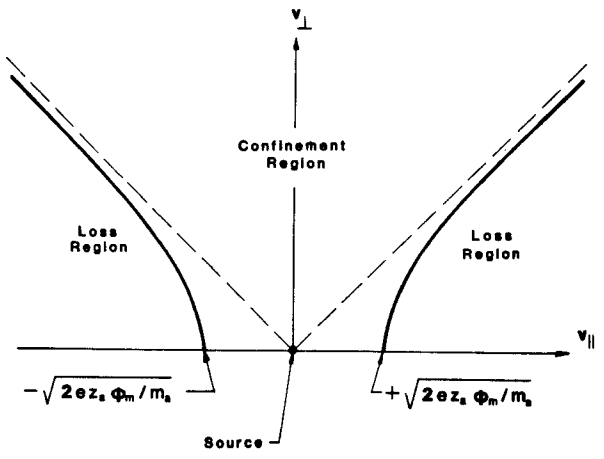

Figure 2.11. *Velocity-space loss region for the Pastukhov problem of particles confined by the combination of an electrostatic potential and a magnetic mirror.*

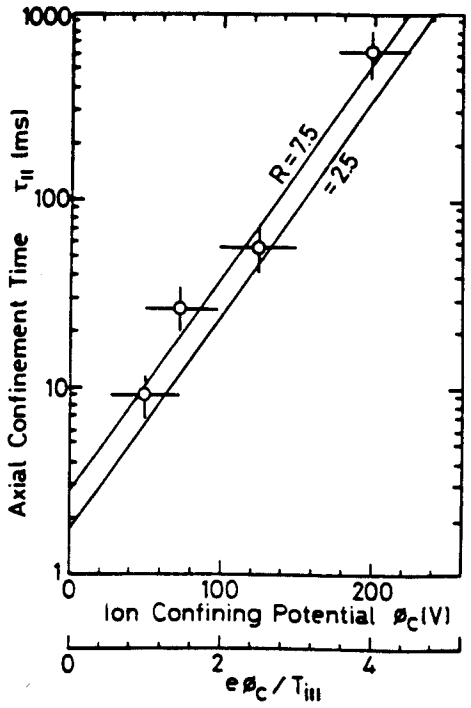

Figure 2.12. *Verification of Pastukhov Loss* $\exp(\Phi/T)$ *dependence in GAMMA-10 [54].*

for the fusion products roughly requires that the axial magnetic field gradient scale length, L_m, satisfy the condition that $L_m \gtrsim v_{\|}/\omega_{ci}^0$, where $v_{\|}$ is the parallel velocity and ω_{ci}^0 is the gyrofrequency at the field minimum [56]. This condition generally does not unduly constrain the design of experiments or reactors. In fact, it may even be useful to enhance the loss of high-energy fusion products and convert them to electricity at high efficiency [57, 58] or use them for specialized purposes such as positron production or fission-waste transmutation [59].

Loss of plugging in TMX-U. The TMX-U experiment experienced a troublesome loss of end plugging at a plasma density of $\sim 3 \times 10^{18}$ m^{-3}. Several explanations have been put forth, but the experiment was terminated before a definitive explanation emerged. Post [1] attributes the difficulties experienced by TMX-U in attempting to achieve high density to an excessively high barrier filling rate, although competing explanations exist. Another strong possibility is that radial $\mathbf{E}\times\mathbf{B}$ drifts were generated in the plugs due to the asymmetric ECRF heating in a highly elliptical magnetic flux tube region [60]. The most worrisome explanation, of course, is an unknown microinstability.

2.4.6 Radial Transport

Although mirror geometry is generally easier to treat theoretically than is tokamak geometry, mirror machines allow different (non-ambipolar) axial and radial loss rates, which somewhat complicate the analysis. It is convenient here to separate mirror devices into two classes: axisymmetric and non-axisymmetric. For axisymmetric devices, 'classical' radial transport occurs for both electrons and ions, with a diffusion coefficient of $D \sim \nu_c \rho^2$, where ν_c is the collision frequency and ρ is the gyroradius. In general, classical radial transport is very small and can be neglected for most practical purposes.

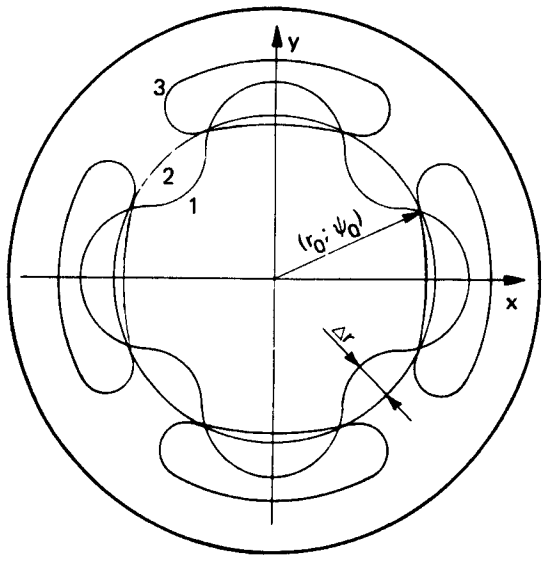

Figure 2.13. *Cross section of typical tandem mirror particle drift surfaces [61].*

For minimum-B tandem mirrors, curvature and gradient drifts due to the non-axisymmetric magnetic flux tubes lead to radial excursions from the flux surfaces. Typical drift surfaces in non-axisymmetric tandem mirrors are shown in Fig. 2.13 [61]. In particular, mirror-trapped particles must see almost cancelling drifts at their turning points, or their transport will be significantly enhanced. This was verified in the GAMMA-6 tandem mirror, where the magnetic flux tube in the central cell was elliptical, leading to additive radial drift contributions and to very large transport rates [62].

One form of non-axisymmetric mirror radial transport is analogous to neoclassical transport in tokamaks [63]: collisions lead to diffusion with radial step sizes that depend on large excursions from flux surfaces rather than on the much smaller gyroradii [64]. 'Banana,' 'plateau,' and 'collisional' collisionality regimes analogous to tokamak neoclassical transport regimes have been delineated, with similar definitions.

The other form of transport important to non-axisymmetric mirrors is caused by radial electric fields that arise in response to either non-

uniform radial plasma profiles or non-ambipolar transport. In this case, the resulting $\mathbf{E}\times\mathbf{B}$ drifts in the azimuthal (Ψ) direction can lead to significant transport losses if either $\Delta\Psi \gtrsim 1$, termed 'resonant' transport, or $\Delta\Psi \gg 1$, termed 'stochastic' transport [65]. Resonant transport is important when $\Delta\Psi$ resonates with a symmetry of the magnetic flux tube geometry, e.g., $\Delta\Psi \simeq \pi/2$ in quadrupole geometry, because the radial drifts then add on each bounce.

Even if the end-region-induced transport loss of particles is manageable, the central cell length in non-axisymmetric tandem mirrors can be limited by transport due to the distortion of central cell flux tubes by parallel currents. These currents occur because the azimuthal curvature and gradient drifts are in opposite direction for ions and electrons. To close the current paths, axial currents must be generated. The minimization of such distortions can be a major design constraint.

2.4.7 Transport Summary

Experiments have demonstrated that electron thermal conduction losses in mirror machines are negligible. The main transport-induced energy loss mechanism is the scattering up in energy of ions or electrons, causing them to be lost over the respective confining electrostatic potential. The theory of this 'Pastukhov' loss problem is well developed, and experiments have verified the theoretical scaling formula. However, the TMX-U experiment experienced a loss of end plugging at plasma densities above $\sim 10^{18}$ m^{-3}, and a definitive explanation does not exist. The most likely explanation for this loss of plugging appears to be azimuthal electrostatic potentials generated by the localized ECRF, with consequent $\mathbf{E}\times\mathbf{B}$ radial drifts.

The creation of thermal barriers, both with and without 'hot' electrons in the barrier regions, is well established. Theoretical treatments exist for the collisional pitch-angle scattering of ions into the thermal barrier, but only the basic scaling has been verified experimentally. A critical need is the experimental demonstration of a thermal barrier pumping mechanism that will work effectively in the reactor regime. The present leading candidate for barrier pumping, ponderomotive-force drift pumping, has no experimental data base.

Non-axisymmetric, minimum-B tandem mirrors can experience significant radial transport losses, particularly due to resonant and stochastic diffusion, where asymmetry-induced radial steps do not cancel at opposite ends of the magnetic mirrors. End cell asymmetry can also induce axial currents which distort the central cell flux surfaces and enhance radial transport. Although radial transport in non-axisymmetric tandem mirrors is reasonably well understood, its effects limit the available design space. In axisymmetric tandem mirrors, only the very small 'classical' collisional transport applies. Thus, a strong transport incentive exists to find suitable axisymmetric configurations.

2.5 Fusion-Product Physics

As for all fusion-reactor configurations, definitive answers to the question of the effects of fusion products must await a thorough experimental test program. This section will summarize the theoretical work that has been accomplished on fusion products in tandem mirrors. There are two main topics of interest: (1) fusion-product particle loss and energy deposition, and (2) instabilities driven by the fusion products. The discussion will focus here on the 3.5 MeV alpha particles generated by D-T reactions and on the 14.7 MeV protons generated by D-^{3}He reactions. The physics of the D-^{3}He alpha particle (3.7 MeV) and of the charged fusion products from D-D reactions will be qualitatively similar to that of the D-T alpha particle.

2.5.1 Fusion-Product Particle Loss and Energy Deposition

Neutral-beam injection experiments indicate that high-energy ions slow down classically on a background plasma, as expected. This allows some confidence in predictions from the relatively simple problem of computing the particle and energy losses as fusion products thermalize in the presence of a loss region. For a given species, there exists a 'critical' energy, $E_c \simeq 30\ T_e$, at which pitch-angle scattering and electron drag are equal in magnitude. Above E_c, electron drag dominates, and little loss of particles to the loss region will occur, except for particles born in the loss cone. The most difficult part of the problem is modelling the boundary between trapped and lost particles. This problem has been solved [66], and typical D-T reactor parameters lead to the prediction that 5–10% of the alpha-particle energy and 10–20% of the alpha particles would be lost during thermalization. Because D-^{3}He protons are born at four times the alpha energy and because of the lower proton mass, their critical energy is only 10–15 T_e, so electron drag dominates for ~95% of their energy loss, and the loss cone has only a small effect.

Because the tandem mirror central cell is typically a long cylinder with a small radius, flat radial density and temperature profiles, such as those required by wall stabilization, can lead to significant energy loss to the plasma halo. The halo is the region between the core plasma and the first wall; it contains a low temperature, fairly high density plasma that can cause significant fusion-product drag. Theoretical models and computer codes exist that give approximate predictions for the losses from this mechanism [67, 36]. The results are very design dependent, but they are expected to be less than 10% of the fusion power, even for wall-stabilized reactors.

2.5.2 Fusion-Product Driven Instabilities

The large gyroradii of fusion products often provide a stabilizing influence on MHD modes. However, there is a mirror loss cone and, consequently, free energy in an anisotropic fusion-product distribution function. Also, the fusion-products can exceed the Alfvén velocity, v_A, in some parameter regimes, which facilitates driving Alfvén waves. A quasilinear theoretical treatment exists for the most dangerous mode, the alpha-loss-cone instability [68]. This theory predicts that the MARS tandem mirror reactor [35] would be unstable to the alpha-loss-cone instability and would require $\lesssim 10\%$ more power to replace the resulting energy losses. Although the design modifications required to offset these losses would probably be modest, there will be a strong incentive to design future tandem mirror reactors in parameter regimes that avoid the alpha-loss-cone instability.

2.5.3 Fusion-Product Physics Summary

Theoretical calculations exist for the important problems of fusion products scattering into the loss cone or interacting with the halo while thermalizing and for the alpha-loss-cone instability. These processes may each lead to effects that could reduce the fusion power available to the core plasma by ~10%. A cumulative 30% effect would substantially reduce the reactor performance, so minimizing these losses must be a major element of future reactor and test facility designs.

2.6 Startup

The startup of the plasma of a conventional tandem mirror was demonstrated successfully in the beginning of the tandem mirror program. Basically, one creates a target plasma by ei-

ther pre-ionization of gas using microwaves or electron beams, or by injecting a plasma from plasma guns at the ends of the machine. Neutral beam injection into the plugs then creates the hot ion plug plasma, which provides the electrostatic confinement and the MHD stabilization of the central cell plasma. Once created, the central cell plasma is sustained by neutral gas puffing in the central cell, although pellet injection or other forms of refuelling are required for a reactor because of the failure of neutral gas to penetrate the larger and hotter plasmas characteristic of reactors.

Startup of thermal barrier tandem mirrors requires careful programming of the various neutral beams and RF sources. If the thermal barrier is created while the central cell plasma is too cold and dense, the increased collision frequency will cause the thermal barrier to fill with trapped ions at a faster rate than the thermal barrier pump beam is capable of removing them. This will cause the thermal barrier to quench and lead to cooling of the hot electrons in the thermal barrier and the plug. One particular startup sequence [69] studied in relation to TMX-U was to first build up a hot electron plasma in the plugs using gas injection and ECRH. Once the hot electron plasma is created, the sloshing ion neutral beams are turned on to produce a sloshing ion population. Application of microwave power at 2 ω_{ce} in conjunction with the thermal barrier pump beams then produces a thermal barrier; microwave power at ω_{ce} produces the confining potential for the central cell. The central cell is heated with ICRF power while its density is raised by gas puffing in order to maintain an acceptably small thermal barrier filling rate. ICRF heating of the central cell is preferable at low central cell density since it leads to bulk ion heating and not tail heating; neutral beam heating can be used once the central cell density has been increased sufficiently.

Variations of the startup scenario above have been accomplished successfully in TMX-U [43]. The use of ICRH in the central cell allowed thermal barrier operation at higher central cell density than was achievable without ICRH. Central cell densities above 3×10^{18} m^{-3} have not been obtained in TMX-U because of loss of plugging; this phenomenon is not understood, but there is data indicating that it is not related to collisional filling of the thermal barrier. Consequently, sustained thermal barrier operation at the design value of the central cell density was not demonstrated in TMX-U. Thermal barriers have been obtained in GAMMA-10 with central cell densities in the high 10^{19} m^{-3} range [70, 71], when a similar startup sequence is used.

Startup scenarios for the inboard thermal barrier [72] and axicell versions of MFTF-B have also been investigated [73] and show that startup of thermal barrier tandem mirrors can be achieved, but careful programming of the various particle and energy sources is required. Reactor studies such as MARS [35] have also considered startup within the context of a particular reactor design and have also concluded that plasma startup, while requiring careful programming of the various particle and energy sources, can be accomplished using the same physics understanding required for the design operating point. In this sense, startup of a tandem mirror plasma is not unlike the startup of some advanced tokamaks where careful control of the plasma current density is required as the density, temperature, and beta are increased.

2.7 Direct Conversion

One of the key advantages of the tandem mirror configuration is that it facilitates the direct conversion of charged-particle fusion energy into electricity. In fact, because the end-loss ions are falling down an electrostatic potential 'hill' of $\sim$10 T_i as they escape, their ratio of peak energy to energy spread is very high—an ideal condition for electrostatic direct conversion. Experimental electrostatic direct converters have achieved efficiencies up to 90%, with the exact value depending upon the configuration and the

energy distribution of the escaping ions. For realistic fusion reactor direct converters, efficiencies of 70–80% appear feasible for the portion of the fusion power that enters the direct converter.

R.F. Post originally proposed the idea of electrostatic direct conversion for minimum-B mirror fusion reactors with highly elliptical magnetic flux tube fans at the ends [10]. A series of electrodes of gradually increasing voltage was envisioned to slow the ion stream and collect ions with energy between a given collector and the following one. Figure 2.14 shows the geometry and the ion trajectories for a 22-stage direct converter that experimentally achieved 87% efficiency [74]. Furthermore, the theoretically predicted efficiency was within a few percent of the experimental value. Related ideas, which rely on perpendicular electric fields and $\mathbf{E} \times \mathbf{B}$ drifts to separate particles by energy, suffer from low power-density limits due to space-charge effects [75], although they may be useful for high-energy protons from D-^{3}He reactions.

An important variant of the original electrostatic direction conversion idea is to insert grids and 'venetian blind' plates held at constant voltage into the magnetic flux tube [76]. A two-stage experimental version is shown schematically in Fig. 2.15. The venetian blinds are parallel to the incident ion beam so that their transparency is high for ions entering the direct converter. Because the applied electric field behind the venetian blinds has a component perpendicular to the incident ion beam, the ions follow parabolic trajectories which cause the venetian blinds to be opaque to backward going ions. Consequently, ions are collected at either the back plate, which is at a high voltage, or at the venetian blinds, which are at a lower voltage. Although the finite opacity of the grids to the ion loss stream limits the efficiency of this concept to slightly less than that of Post's original concept, the gridded configuration works with flux tubes of arbitrary cross-section, making it more suitable for a variety of tandem mirror configurations, including the important class of axisymmetric devices. Again, theory and experiment agreed within a few percent [11].

Electrostatic direct converters have been tested successfully both on the test stand and on the TMX experiment [11]. A single-stage, gridded direct converter placed in the TMX end-loss stream had a measured efficiency of 48% and a theoretically calculated efficiency of 47%. For D-^{3}He tandem mirror reactors, theory predicts direct converter efficiencies of ~80% [77]. The ability of tandem mirrors to utilize highly efficient direct electrostatic converters is a key advantage for the configuration, particularly with advanced fuels such as D-^{3}He, where almost all of the fusion energy goes to charged particles.

2.8 Conclusions

Mirror and tandem mirror research through 1986 had achieved a good understanding of MHD equilibrium and stability, microstability, and transport physics. However, only four thermal barrier tandem mirror experiments had been operated, and some outstanding issues remained.

High $\bar{\beta}$ values (15–20%) had been routinely reached in tandem mirrors, but theoretical predictions of even higher limits ($\bar{\beta} \sim 80\%$) had not been testable because of limited power in those experiments. Several concepts that would allow very high $\bar{\beta}$ values in *axisymmetric* tandem mirrors had been proposed, and testing of RF stabilization had begun.

The theoretical understanding and experimental elimination of microinstabilities had been accomplished up to the maximum parameters the experiments could reach. Although these modes constrain the operating space, microstable reactor designs appear to be possible without a significant reduction in performance.

The existence of the thermal barrier configuration had been demonstrated, and a fair under-

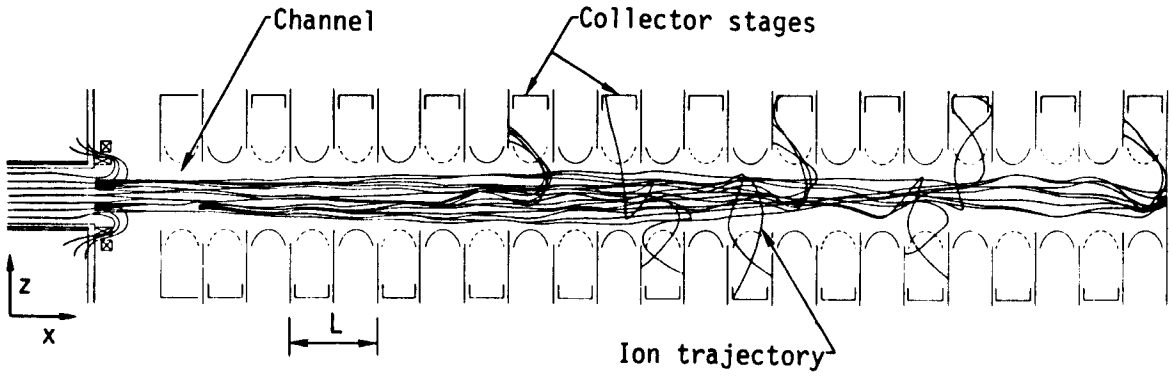

Figure 2.14. *Ion trajectories and configuration of a 22-stage direct converter based on the original concept of Post [74].*

standing of the physics of thermal barrier collisional filling and of possible barrier pumping mechanisms had been reached. The interaction of ECRF with both hot and warm electrons in the barrier and plug region had been examined, but required more extensive testing.

Axial end loss could be predicted with fair confidence up to central cell plasma densities of $\sim 3 \times 10^{18}$ m^{-3}, but a loss of end plugging occurred in TMX-U at higher densities and was not understood. The basic end-loss scaling had received preliminary verification in GAMMA-10 and TMX-U. Radial transport was recognized as capable of causing problems in some parameter regimes for minimum-B stabilized tandem mirrors, particularly because ECRF power is required in regions with non-circular magnetic flux tubes. Azimuthally symmetric tandem mirrors were not expected to experience significant radial transport unless the plug and barrier ECRF power was applied very asymmetrically.

The mechanisms by which fusion products slow down on the background plasma and the plasma halo were fairly well understood theoretically. A microinstability induced by the fusion-product loss cone, the 'alpha-loss-cone' instability, was theoretically predicted to constrain the allowed operating space for reactors.

The startup of tandem mirror experiments had been accomplished successfully, but it was a relatively complex process. Careful programming in time was required for the neutral beam power, the RF power, and the particle fueling sources. Viable startup routes had been defined for conceptual tandem mirror reactor designs.

The outstanding issues indicated above needed to be addressed by an experimental test program and possibly by revisions of theory. Nevertheless, the substantial progress by 1986, both in experimental results and in theoretical understanding, gave considerable confidence that the hurdles could be overcome. Solutions to the remaining problems, particularly if viable, high-β, axisymmetric designs could be found, were recognized to lead to exceptionally attractive magnetic fusion reactors that could burn either D-T or D-^{3}He fuel.

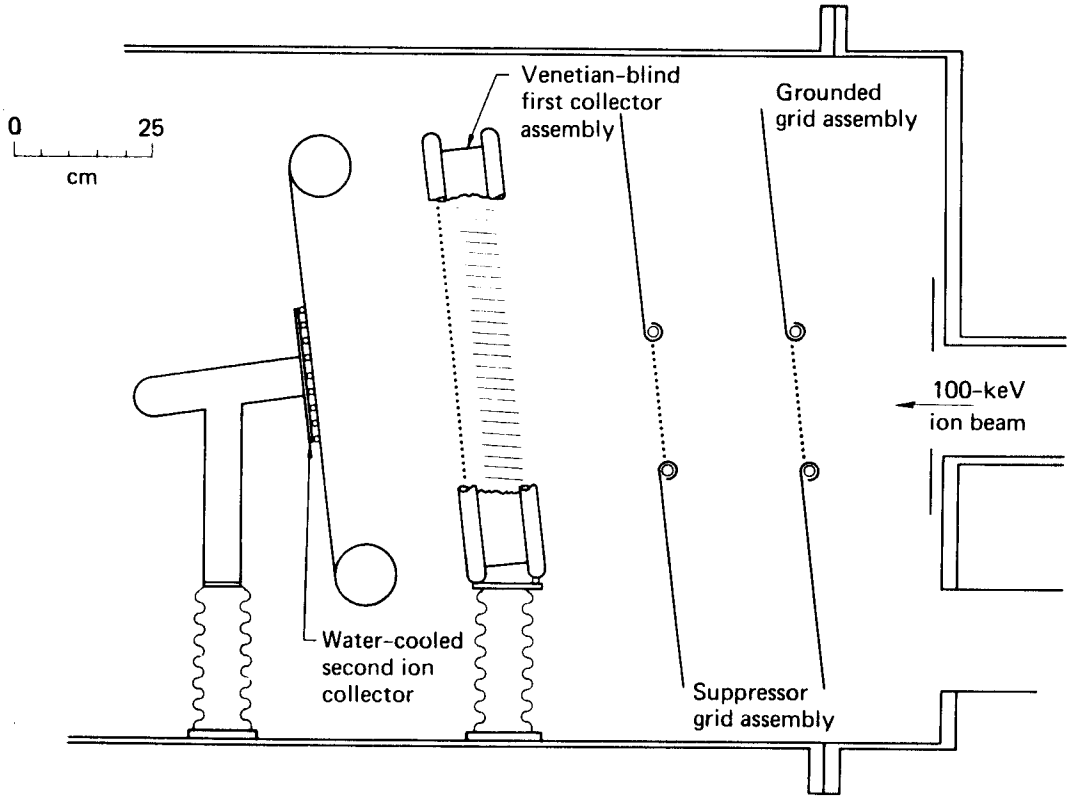

Figure 2.15. *Schematic view of an experimental gridded direct converter [11].*

References for Chapter 2

[1] R.F. Post, "The Magnetic Mirror Approach to Fusion," *Nuclear Fusion* **27**, 1579 (1987).

[2] J.D. Callen, J.F. Santarius, D.E. Baldwin, R.D. Hazeltine, R.K. Linford, et al., *TPA Plasma Science Status Report* (University of Wisconsin Report, December, 1986).

[3] J. Kesner, M.J. Gerver, B.G. Lane, B.D. Lane, R.E. Aamodt et al., "Introduction to Tandem Mirror Physics," Massachusetts Institute of Technology Report PFC/RR-83-35 (1983).

[4] B.I. Cohen, editor, "Status of Mirror Fusion Research 1980," Lawrence Livermore National Laboratory Report UCAR 10049-80-Rev. 1 (1980).

[5] C. Gormezano, "Reduction of Losses in Open-Ended Magnetic Traps," *Nuclear Fusion* **19**, 1085 (1979).

[6] D.E. Baldwin, "End-Loss Processes from Mirror Machines," *Rev. Mod. Phys.* **49**, 317 (1977).

[7] T.K. Fowler, "Fusion Research in Open-Ended Systems," *Nuclear Fusion* **9**, 3 (1969).

[8] A.S. Bishop, *Project Sherwood: The U.S. Program in Controlled Fusion* (Addison-Wesley, Massachusetts, 1958).

[9] R.F. Post, "Controlled Fusion Research—An Application of the Physics of High Temperature Plasmas," *Rev. Mod. Phys.* **28**, 338 (1956).

[10] R.F. Post, "Mirror Systems: Fuel Cycles, Loss Reduction and Energy Recovery," *British Nuclear Energy Society Fusion Reactor Conference* (Culham Laboratory, England), p. 88 (1969).

[11] W.L. Barr and R.W. Moir, "Test Results on Plasma Direct Converters," *Nuclear Technology/Fusion* **3**, 98 (1983).

[12] G.I. Dimov, V.V. Zakaidakov, and M.E. Kishinevsky, "Thermonuclear Confinement with Twin Mirror Systems," *Fiz. Plasmy* **2**, 597 (1976) [*Sov. J. Plasma Phys.* **2**, 326 (1976)].

[13] T.K. Fowler and B.G. Logan, "The Tandem Mirror Reactor," *Comments on Plasma Physics and Controlled Fusion* **2**, 167 (1977).

[14] D.E. Baldwin and B.G. Logan, "Improved Tandem Mirror Fusion Reactor," *Phys. Rev. Lett.* **43**, 1318 (1979).

[15] B.V. Chirikov, "A Universal Instability of Many-Dimensional Oscillator Systems," *Physics Reports* **52**, 263 (1979).

[16] L.S. Hall and B. McNamara, "Three-Di mensional Equilibrium of the Anisotropic, Finite-Pressure Guiding-Center Plasma: Theory of the Magnetic Plasma," *Phys. Fluids* **18**, 552 (1975).

[17] W.C. Turner, J.H. Clauser, F.H. Coengsen, D.L. Correll, W.F. Cummins, et al., "Field-Reversal Experiments in a Neutral-Beam-Injected Mirror Machine," *Nuclear Fusion* **19**, 1011 (1979).

[18] H.L. Berk, M.N. Rosenbluth, H.V. Wong, T.M. Antonsen, and D.E. Baldwin, "Fast

Growing Trapped-Particle Modes in Tandem Mirrors," *Sov. J. Plasma Phys.* **9**, 108 (1983).

[19] T.C. Simonen, editor, "Summary of the Results from the Tandem Mirror Experiment (TMX)," Lawrence Livermore National Laboratory Report UCRL-53120 (1981).

[20] J.R. Ferron, N. Hershkowitz, R.A. Breun, S.N. Golovato, and R. Goulding, "RF Stabilization of an Axisymemetric Tandem Mirror," *Phys. Rev. Lett.* **51**, 1955 (1983).

[21] R.A. Breun, P. Brooker, D.A. Brouchous, J. Browning, G. Butz, et al., "Stabilization of MHD Modes in an Axisymmetric Magnetic Mirror by Applied RF Waves and Initial Results of Phaedrus-B," in *Plasma Physics and Controlled Nuclear Fusion Research 1986, Vol. 2*, p. 263 (IAEA, Vienna, 1987).

[22] D.A. D'Ippolito and J.R. Myra, "Quasilinear Theory of the Ponderomotive Force: Induced Stability and Transport in Axisymmetric Mirrors," *Phys. Fluids* **28**, 1895 (1985).

[23] D.A. D'Ippolito and J.R. Myra, "Stabilization of Magnetohydrodynamic Modes by Applied Radio-Frequency Waves," *Phys. Fluids* **29**, 2594 (1985).

[24] J. Kesner, "Axisymmetric, Wall-Stabilized Tandem Mirrors," *Nuclear Fusion*, **25**, 275 (1985).

[25] R.A. Close, B.K. Kang, A.J. Lichtenberg, M.A. Lieberman, and H. Meuth, "Experimental Observation of Stabilization of an Axisymmetric Mirror at High Beta with a Nearby Wall," *Phys. Fluids* **29**, 3892 (1986).

[26] J. Kesner, B. Lane, and R.S. Post, "Stabilization of MHD Modes in an Axisymmetric Column through the Use of a Magnetic Diverter," *Nuclear Fusion* **27**, 217 (1987).

[27] F.L. Hinton and M.N. Rosenbluth, "Stabilization of Axisymmetric Mirror Plasmas by Energetic Ion Injection," *Nucl. Fusion* **22**, 1547 (1982).

[28] I.A. Kotel'nikov, G.V. Roslyakov, D.D. Ryutov, and G.V. Stupakov, "Stabilization of Flute Instability in Axially Symmetric Mirror Machines," in *Plasma Physics and Controlled Nuclear Fusion Research 1986, Vol. 2*, p. 305 (IAEA, Vienna, 1987).

[29] R.S. Post, K. Brau, J. Casey, J. Coleman, M. Gerver, et al., "Stability Issues in the Tara Tandem Mirror Experiment," in *Plasma Physics and Controlled Nuclear Fusion Research 1988, Vol. 2*, p. 493 (IAEA, Vienna, 1989).

[30] J. Kesner, R.S. Post, B.D. McVey, and D.K. Smith, "A Tandem Mirror with Axisymmetric Central-Cell Ion Confinement," *Nucl. Fusion* **22**, 549 (1982).

[31] G.D. Porter, editor, *TMX-U Final Report, Vols. 1 and 2*, Lawrence Livermore National Laboratory Report UCID-20981, Vol. 1 and 2 (1988).

[32] D.E. Baldwin, H.L. Berk, and L.D. Pearlstein, "Turbulent Lifetimes in Mirror Machines," *Phys. Rev. Lett.* **36**, 1051 (1976).y

[33] T. Cho, M. Ichimura, M. Inutake, et al., "Studies of Potential Formation and Transport in the Tandem Mirror GAMMA-10," in *Plasma Physics and Controlled Nuclear Fusion Research 1986, Vol. 2*, p. 243 (IAEA, Vienna, 1987).

[34] B. Badger, K. Audenaerde, J.B. Beyer, D. Braun, J.D. Callen, et al., "WITAMIR-I: A University of Wisconsin Tandem Mirror Reactor Design," University of Wisconsin Report UWFDM-400 (1980).

[35] B.G. Logan, C.D. Henning, G.A. Carlson, R.W. Werner, D.E. Baldwin, et al., *MARS: Mirror Advanced Reactor Study*, Lawrence Livermore National Laboratory Report UCRL-53480 (1984).

[36] J.D. Lee, Technical Editor, *MINIMARS Conceptual Design: Final Report*, Lawrence Livermore National Laboratory Report UCID-20773, Vols. I and II (1986).

[37] A.H. Futch and L.L. LoDestro, "Collisional Trapping Rates for Ions in a Magnetic and Potential Well," Lawrence Livermore National Laboratory Report UCRL-87249 (1982).

[38] R. Carrerra and J.D. Callen, "Thermal Barrier Ion Trapping Rate in a Tandem Mirror," *Nucl. Fusion* **23**, 433 (1983).

[39] X.Z. Li and G.A. Emmert, "A Variational Calculation of the Trapping Rate in Thermal Barriers," *Nucl. Fusion* **24**, 359 (1984).

[40] Li Xingzhong and G.A. Emmert, "Analytical Expression for Trapped-Particle Current in Thermal Barrier of a Tandem Mirror," *Scientia Sinica (A)* **29**, 604 (1986).

[41] R.S. Devoto, L.L. LoDestro, and A.A. Mirin, "Trapping Rates in Thermal Barriers of Tandem Mirrors," *Nucl. Fusion* **27**, 255 (1987).

[42] P.J. Catto and R. Carrera, "Particle Exchange in the Plug of a Thermal Barrier Tandem Mirror," *Phys. Fluids* **26**, 2161 (1983).

[43] D.P. Grubb, S.L. Allen, T.A. Casper, J.F. Clauser, F.H. Coensgen, et al., "Thermal-Barrier Production and Identification in a Tandem Mirror," *Phys. Rev. Lett.* **53**, 783 (1984).

[44] D.E. Baldwin, J.A. Byers, Y.J. Chen, and T.B. Kaiser, "Drift Pumping of Tandem Mirror Thermal Barriers," in *Plasma Physics and Controlled Nuclear Fusion Research 1986, Vol. 2*, p. 293 (IAEA, Vienna, 1987).

[45] M. Rosenberg, N.A. Krall, and J.B. McBride, "Wave-Induced Plasma Transport in the Magnetic Drift Frequency Range," *Phys. Fluids* **28**, 538 (1985).

[46] Y. Yasaka and R. Itatani, "Convective Plasma Loss Caused by an Ion-Cyclotron RF Field and Its Elimination by Mode Control," *Phys. Rev. Lett.* **44**, 1763 (1980).

[47] J.F. Santarius and J.D. Callen, "Ponderomotive Force Pumping of Tandem Mirror Thermal Barriers," Sherwood Theory Meeting (1985).

[48] N. Hershkowitz, B.A. Nelson, J.R. Ferron, R.H. Goulding, and E. Wang, "ICRF Produced Thermal Barriers in a Three-Cell Axisymmetric Tandem Mirror," *Nucl. Fusion* **28**, 1333 (1988).

[49] R.H. Cohen, I.B. Bernstein, J.J. Dorning, and G. Rowlands, "Particle and Energy Exchange between Untrapped and Electrostatically Confined Populations in Magnetic Mirrors," *Nucl. Fusion* **20**, 1421 (1980).

[50] V.P. Pastukhov, "Collisional Losses of Electrons from an Adiabatic Trap in a Plasma with a Positive Potential," *Nucl. Fusion* **14**, 3 (1974).

[51] R.H. Cohen, M.E. Rensink, T.A. Cutler, and A.A. Mirin, "Collisional Loss of Electrostatically Confined Species in a Magnetic Mirror," *Nucl. Fusion* **18**, 1229 (1978).

[52] P.J. Catto and I.B. Bernstein, "Collisional End Losses from Conventional and Tandem Mirrors," *Phys. Fluids* **24**, 1900 (1981).

[53] F. Najmabadi, R.W. Conn, and R.H. Cohen, "Collisional End Loss of Electrostatically Confined Particles in a Magnetic Mirror Field," *Nucl. Fusion* **24**, 75 (1984).

[54] M. Inutake, T. Cho, M. Ichimura, K. Ishii, A. Itakura, et al., "Thermal Barrier Formation and Plasma Confinement in the Axisymnmetrized Tandem Mirror GAMMA 10," *Phys. Rev. Lett.* **55**, 939 (1985).

[55] B.G. Logan, A.A. Mirin, and M.E. Rensink, "An Analytic Model for Classical

Ion Confinement in Tandem Mirror Plugs," *Nucl. Fusion* **20**, 1613 (1980).

[56] R.H. Cohen, G. Rowlands, and J.H. Foote, "Nonadiabaticity in Mirror Machines," *Phys. Fluids* **21**, 627 (1978).

[57] J.F. Santarius, "Very High Efficiency Fusion Reactor Concept," *Nucl. Fusion* **27**, 167 (1987).

[58] J.F. Santarius, H.M. Attaya, M.L. Corradini, L.A. El-Guebaly, G.A. Emmert, et al., "Ra: A High Efficiency, D-^{3}He, Tandem Mirror Fusion Reactor," *Twelfth Symposium on Fusion Engineering*, p. 752 (IEEE, NY, 1987).

[59] J.M. Dawson, "Nonenergy Applications for Fusion," *Fusion Technol.* **22**, 99 (1992).

[60] G. Dimonte, "Radial Transport in a Tandem Mirror," *Phys. Rev. Lett.* **60**, 1390 (1988).

[61] M.E. Kishinevskij, P.B. Lysyanskij, D.D. Ryutov, G.V. Stupakov, B.M. Fomel', et al., "Transverse Particle Losses in Axially Asymmetrical Open Traps," in *Plasma Physics and Controlled Nuclear Fusion Research 1978, Vol. 2*, p. 411 (IAEA, Vienna, 1979).

[62] K. Yatsu, et al., "Radial Plasma Confinement Time in the Central Cell of GAMMA 6 Determined from Measurement with a Charge Collector," *Jap. J. Appl. Phys.* **20**, L601 (1981).

[63] F.L. Hinton and R.D. Hazeltine, "Theory of Plasma Transport in Toroidal Confinement Systems," *Rev. Mod. Phys.* **48**, 239 (1976).

[64] D.D. Ryutov and G.V. Stupakov, "Neoclassical Transport in Ambipolar Confinement Systems," *Fiz. Plazmy* **4**, 501 (1978) [*Sov. J. Plasma Phys.* **4**, 278 (1978)].

[65] D.D. Ryutov and G.V. Stupakov, "Diffusion of Resonance Particles in Ambipolar Plasma Traps," *Dokl. Akad. Nauk SSSR* **240**, 1086 (1978) [*Sov. Phys. Dokl.* **23**, 412 (1978)].

[66] H. Hamnén and J.D. Hanson, "The Fast-Alpha-Particle Distribution Function in an Open-Field-Line Plasma with Electrostatic Confining Potential," *Nucl. Fusion* **25**, 1451 (1985).

[67] J.F. Santarius, "Halo Plasma Physics Model for Mirror Machines with Neutral Beam Injection," *Nucl. Fusion* **26**, 887 (1986).

[68] S.K. Ho, G.R. Smith, and G.H. Miley, "Quasilinear Diffusion Modeling of the Alpha-Loss-Cone Instability in a Tandem-Mirror Reactor," *Phys. Fluids* **B1**, 2040 (1989).

[69] A.W. Molvik and S. Falabella, "Use of ICRH for Startup and Initial Heating of the TMX-U Central Cell," Lawrence Livermore National Laboratory Report UCID-19342 (1982).

[70] T. Cho, M. Ichimura, M. Inutake, et al., "Potential Formation in Axisymmetrized Tandem Mirror GAMMA 10," *Plasma Physics and Controlled Nuclear Fusion Research 1984, Vol. 2*, p. 275 (IAEA, Vienna, 1985).

[71] S. Miyoshi, T. Cho, H. Hojo, et al., "Development of Tandem Mirror Experiments in GAMMA-10," *Plasma Physics and Controlled Nuclear Fusion Research 1990, Vol. 2*, p. 539 (IAEA, Vienna, 1991).

[72] J.M. Gilmore, "Plasma Buildup in Tandem Mirror Machines," Ph.D. thesis, Department of Nuclear Engineering and Engineering Physics, University of Wisconsin, Madison, WI (1980).

[73] E. Montalvo and G. Emmert, "Time Dependent Studies of a Tandem Mirror with Thermal Barriers," *Nuclear Fusion* **26**, 1003 (1986).

[74] W.L. Barr, R.W. Moir, and J.D. Kinney, "Experimental and Computational Results on Direct Energy Conversion for Mirror Fusion Reactors," *Nucl. Fusion* **17**, 1015 (1977).

[75] W.L. Barr, "Direct Energy Recovery from a Beam of Charged Particles Using Parabolic Ion Trajectories," Lawrence Livermore National Laboratory Report UCRL-51147 (1971).

[76] R.W. Moir and W.L. Barr, " 'Venetian-Blind' Direct Energy Converter for Fusion Reactors," *Nucl. Fusion* **13**, 35 (1973).

[77] R.F. Post and J.F. Santarius, "Open Confinement Systems and the D-^{3}He Reaction," *Fusion Technol.* **22**, 13 (1992).

Chapter 3

Tandem Mirror Physics Progress Since 1986

3.1 Introduction

This chapter surveys the progress made in tandem mirror physics since the TMX-U experiment—the major part of the U.S. fusion research program—was shut down in 1986. During this time period, ~200 papers related to tandem mirrors were published in refereed journals. A brief evaluation of what were judged to be the most important of these papers was performed, but an exhaustive study of all of them was not possible within the resources of the present project.

This chapter is organized into topics that parallel those in the main sections of Chapter 2. Some of the material in this chapter discusses new experiments on the thermal barrier tandem mirrors that have continued operating, especially on GAMMA-10 and Phaedrus, while other material describes further analysis of data taken earlier on TMX-U. A section on fuel cycles for tandem mirror reactors has been added, because interest in this topic has revived since 1986 due to the identification of the lunar ^{3}He resource [1].

3.2 MHD Equilibrium and Stability

3.2.1 Equilibrium

MHD equilibrium theory for tandem mirrors can be considered to be well established. The main equilibrium result since 1986 has been the further verification of the electrostatic potential structure in GAMMA-10 [2].

3.2.2 Minimum-B MHD Stability

The main result during this period in the area of minimum-B stability is that the TMX-U experiment published an analysis of earlier experimental results in which the central β limit that was below the standard MHD limit by about a factor of six [3]. These experiments were run in the original tandem mirror configuration, with quadrupole end cells and without thermal barriers. There are difficulties in interpreting these results, however; they have, for example, been interpreted as drift-wave turbulence due to an unknown microinstability [3].

3.2.3 Axisymmetric MHD Stability

As discussed in Sec. 2.2.3, several ideas for stabilizing axisymmetric tandem mirrors were

emerging in 1986: RF stabilization, magnetic divertor stabilization, wall stabilization, sloshing-ion stabilization, and non-paraxial mirror stabilization. Those which were the subject of further research since 1986 are discussed below. They have received varying degrees of development and experimental verification.

Most of the effort on achieving axisymmetric tandem mirror operation has been in the *RF stabilization* area. An excellent theoretical understanding of RF stabilization had been developed through 1986, as discussed in Sec. 2.2.3. Much of the experimental effort since that time has been spent testing the theory, with reasonable agreement found. Extensive results from the Phaedrus experiment were published [4, 5, 6, 7], and Tara [8] also achieved stable axisymmetric operation using ICRF.

Some refinements of *wall-stabilization* theory were made after 1986 [9, 10]. In particular, it was shown that central-cell magnetic-field ripple—which usually contributes destabilizing terms to the MHD analysis—helps in the wall-stabilized case [10].

Experimental results from the Tara experiment indicated that *magnetic divertors* helped the MHD stability [11], as predicted by theory, although the exploration of parameter space was limited by the presence of the trapped-particle mode discussed below.

3.2.4 Trapped-Particle Modes

The localized, electrostatic trapped-particle mode was identified in Tara, and reasonably good agreement with theory was found [12]. The mode may also have been observed in TMX-U [13]. A later paper discussed this TMX-U low-frequency instability, and concluded that it may have been driven instead by $\mathbf{E}\times\mathbf{B}$ rotation, although a definite identification was not possible [14].

On the theoretical side, some further work on the trapped-particle mode found that it would be possible, in principle, to stabilize it 'robustly' in tandem mirrors [15]. A Fokker-Planck code for analyzing the mode was also written [16]. Thus, the trapped-particle mode appears to constrain design space, but the tools are available to predict and avoid its occurrence.

3.2.5 MHD Summary

Very little occurred during this time period in the areas of equilibrium or minimum-B stability. Significant, encouraging extensions were made in the experimental operation and theoretical understanding of axisymmetric tandem mirrors, especially for RF, wall, and magnetic-divertor stabilization. The trapped-particle mode appears to have been identified, as expected, in the Tara configuration, while its identification in TMX-U is uncertain.

3.3 Microstability

3.3.1 Overview

There may have been an observation of a drift wave in the TMX-U experiment [3], but the identification of the mode was ambiguous. Some early work on tandem mirror drift waves had been done [17], but they have not yet been positively identified. It is not presently clear how much they would constrain the tandem mirror reactor operating space.

3.3.2 DCLC and AIC Modes

These modes were well understood prior to 1987, and little work has been done on them since that time.

3.3.3 Microstability Summary

Tandem mirror experiments have generally operated with very low levels of fluctuations that can be attributed to microinstabilities. This area has only been slightly active since 1986.

3.4 Transport

3.4.1 Electron Thermal Conduction

This topic is no longer an issue for mirror devices with plasma temperatures beyond a few 10's of eV.

3.4.2 Electrostatic Potentials

The basic physics of the thermal barrier tandem mirror electrostatic potential formation has not been questioned during this period.

3.4.3 Thermal Barrier Physics

Thermal barrier collisional filling In the TMX-U experiment, ICRF power was used to heat the passing ions and reduce their collisionality by about a factor of ten [18]. This did not, however, allow TMX-U to reach higher densities, indicating that collisional barrier filling was not related to the loss-of-plugging problem.

Thermal barrier pumping The concept of ponderomotive-force pumping of thermal barriers was demonstrated to be possible in relatively small experiments [5, 19]. A related thermal-barrier pumping method, using the $\mu\nabla B$ force on a magnetic-field slope, was observed in the Phaedrus experiment [20].

Thermal barrier electrostatic potential Further verification of the existence of thermal barrier potentials occurred in GAMMA-10 [2] and Phaedrus [21]. Fig. 3.1 shows the measured axial profiles of electrostatic potential, plasma density, and magnetic field for the Phaedrus experiment during thermal-barrier operation [21].

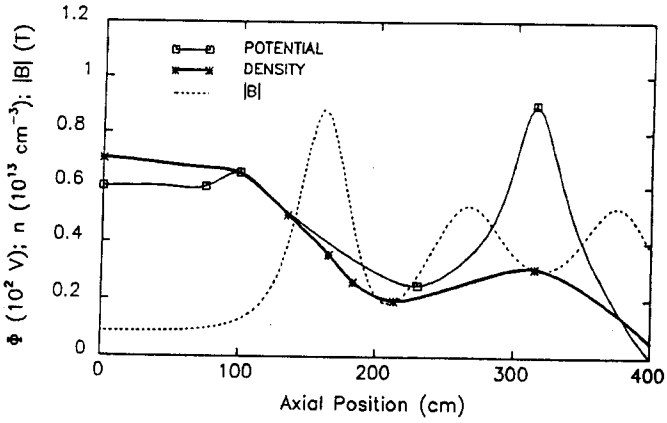

Figure 3.1. *Axial profiles of the electrostatic potential, plasma density, and magnetic field for the Phaedrus experiment [21].*

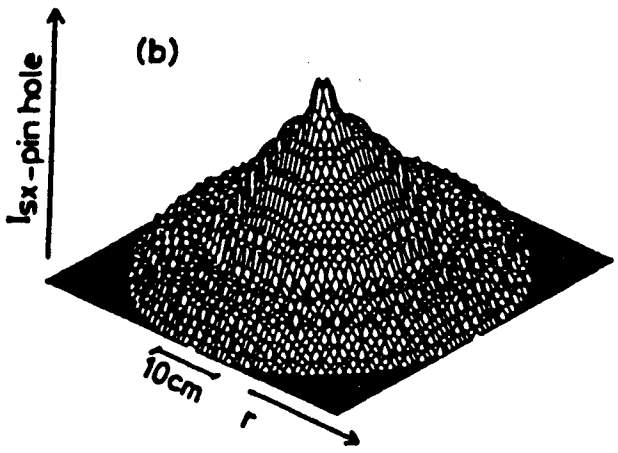

Figure 3.2. *Radial profile of the hot electrons in the thermal barrier of GAMMA-10 [22].*

The GAMMA-10 experiment also demonstrated the existence of the hot-electron 'disk' necessary to the efficient functioning of the thermal barrier when both the barrier and plug are in a single cell [22]. A typical radial profile of the hot electrons is shown in Fig. 3.2.

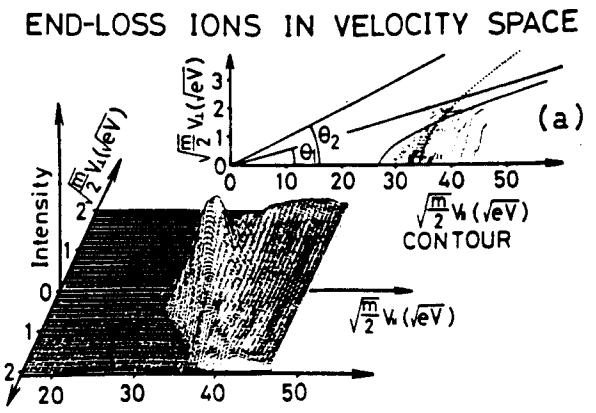

Figure 3.3. *End-loss energy spectrum in GAMMA-10 [25].*

3.4.4 Axial Loss

Some progress has been made since 1986 in understanding the loss of end-plugging experienced by TMX-U for densities about 3×10^{18} m^{-3} [23]. Central-cell ICRF heating experiments in TMX-U increased the central cell ion temperature and reduced thermal barrier trapping of the passing ions, but this did not remove the limitation on central cell density [18]. The implication is that the loss of end plugging is not due to barrier trapping. A likely explanation for the loss of plugging has been given by Dimonte [24]. That is, ECRF heating in the highly elliptical end-plug magnetic flux tubes creates azimuthal potential structures, and the resultant azimuthal **E** fields induce **E**×**B** radial drifts. Even more importantly, the GAMMA-10 and Phaedrus experiments were able to operate with strong end plugging at densities of $\gtrsim 10^{19}$ m^{-3}, including the suppression of both axial and radial losses.

The Pastukhov end-loss scaling was verified further during this time [2], and the GAMMA-10 experiment observed an end-loss-ion energy distribution that graphically shows the expected velocity-space loss region [25] (see Fig. 3.3).

3.4.5 Radial Transport

Except for RF-induced radial transport, discussed earlier, there has been little activity in this area since 1986.

3.4.6 Transport Summary

Generally, the formation of electrostatic potentials in tandem mirrors is well understood, but questions remain regarding the rate of thermal barrier collisional filling. Thermal barrier pumping mechanisms, especially ponderomotive-force pumping, have received preliminary verification, but experiments must be performed at reactor-relevant parameters. The limit on central cell density due to the loss of end plugging in TMX-U has been tentatively explained as due to **E**×**B** drifts. Pastukhov end-loss scaling can be considered to be well verified, the basic scaling having been observed over three orders of magnitude.

3.5 Fusion-Product Physics

3.5.1 Fusion-Product Particle Loss and Energy Deposition

This area has not received any attention since 1986.

3.5.2 Fusion-Product Driven Instabilities

An important development in this area was the theoretical analysis of the 'alpha-loss-cone' mode, which results when an Alfvén wave is driven by the fusion product loss cone [26, 27]. This research predicts that the MARS conceptual reactor design [28] would have lost 36% of its alpha particles and 47% of its alpha-particle energy [27], a prohibitive energy loss. Although

the theory of the alpha-loss-cone instability is not yet well developed, these results give serious concern and would require significant modification of the MARS design if they remain valid.

3.5.3 Fusion-Product Physics Summary

The key development since 1986 in this area is the theoretical analysis of the alpha-loss-cone mode, which must be evaluated carefully for future reactor designs and for reactor-relevant experiments.

3.6 Startup

A brief review of the tandem mirror literature since 1986 did not turn up any references to startup issues. There may be some information contained in more general papers primarily describing other results of the various tandem mirror experiments. In particular, careful attention to details of the startup process appear to have helped the GAMMA-10 experiment achieve its success in verifying several aspects of tandem mirror operation [29].

3.7 Direct Conversion

Already prior to 1987, experiments had extensively verified electrostatic direct converter theory and had successfully demonstrated the operation of these devices at high efficiency (see Sec. 2.7). One notable later development was a very detailed, 2-dimensional computer code for electrostatic direct converter analysis [30]. This code verified the earlier, simpler analysis [31].

3.8 Fuel Cycles

This section has no parallel in Chapter 2, because it discusses general fuel-cycle issues in tandem mirrors, rather than primarily reporting the results of previous research.

Although D-T fuel is the easiest to ignite, there are advantages to some of the 'advanced' fuels and, in particular, the D-^{3}He fuel cycle. This is especially true for the tandem mirror, which is well situated to burn D-^{3}He fuel. The difficulty with the D-^{3}He fuel cycle, of course, is in acquiring the ^{3}He fuel, and it presently appears that it will be necessary to rely upon the development of the lunar ^{3}He resource on a relevant time scale [1].

In assessing fusion fuel cycles, no single figure of merit can adequately encompass the multitude of important criteria involved. The cost of electricity is a key reactor parameter, but safety and environmental features will be just as important to the long-term future of fusion power in the marketplace. Furthermore, although the physics figures of merit, such as the fusion power density in the plasma, are easiest to calculate, the engineering features of the device are at least as important.

The two key fusion fuel cycles are expected to be D-T and D-^{3}He. Their main and secondary reactions are given in Table 3.1. The corresponding Maxwellian-averaged reaction rates are shown in Fig. 3.4. The resulting fusion power density in the plasma appears in Fig. 3.5, and the required ignition parameter, $n_e\tau_E$, is plotted in Fig. 3.6. Clearly, D-T fuel has the highest fusion power density in the plasma and will be easiest to ignite.

Turning to *engineering* considerations, the picture is somewhat different. In this case, the difficulties caused by neutrons are a prominent factor, and the attractiveness of D-^{3}He fuel is enhanced because it facilitates the use of charged particles for direct conversion of fusion power to electricity at high efficiency, as discussed in

Table 3.1. *D-T, D-^{3}He, and D-D fusion reactions.*

D +T	→	n (14.07 MeV)+^{4}He (3.52 MeV)
D +^{3}He	→	p (14.68 MeV)+^{4}He (3.67 MeV)
D +D	→	n (2.45 MeV)+^{3}He (0.82 MeV)
D +D	→	p (3.02 MeV)+T (1.01 MeV)

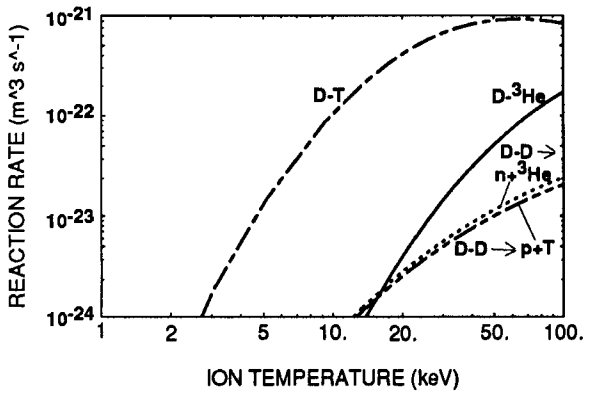

Figure 3.4. *Maxwellian-averaged fusion reaction rates for the reactions most important in D-T and D-^{3}He reactors.*

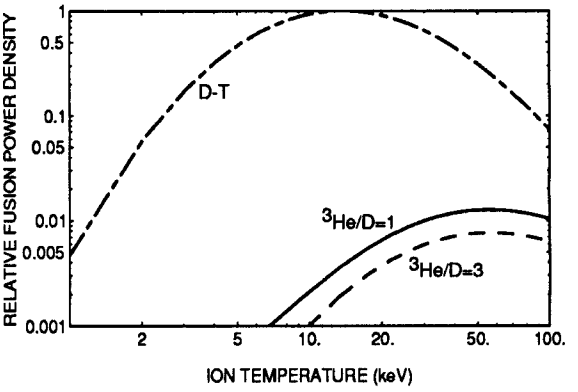

Figure 3.5. *Fusion power density in the plasma for the D-T and D-^{3}He fuel cycles, with two ratios of ^{3}He to D density shown.*

Sec. 2.7. A key engineering figure of merit is the fraction of fusion power produced in neutrons, shown in Fig. 3.7. The neutron power fraction for D-^{3}He can be seen to be reduced far below the D-T value, ameliorating the neutron problems and allowing more charged-particle power for direct conversion.

Rather than the plasma fusion power density, a better figure of merit is the engineering fusion power density, the electric power produced per unit mass of the reactor core—although this is still not a perfect measure. Factors such as the shielding thickness and the limits to surface and neutron heat loads must be considered in this case. A rough comparison between D-T and D-^{3}He can be gained from Table 3.2, which compares the approximate factors involved in the engineering power density for typical D-T and D-^{3}He tandem mirror reactors. The most important point to be drawn from Table 3.2 is that, despite the different fuel cycles, the engineering power density values are about the same. In addition, a D-^{3}He tandem mirror reactor would possess significant safety and environmental advantages, and the complicated tritium-breeding blanket would be eliminated.

3.9 Conclusions

Detailed conceptual designs indicate that attractive tandem mirror reactors can be based on the D-T fuel cycle. Tandem mirrors would also be ideal devices for burning D-^{3}He fuel, because their central cell magnetic field is low and they can greatly increase the fusion power density by increasing the field, they allow efficient electrostatic direct conversion, and they provide high β. D-^{3}He tandem mirror reactors would require higher energy (~2 MeV) neutral beams, but would otherwise be very similar to D-T tandem mirror reactors.

Table 3.2. *Approximate effects on engineering power density for a D-^{3}He tandem mirror reactor compared to a D-T tandem mirror reactor.*

AREA	D-T	D-^{3}He	Effect
Normalized fusion power density in plasma	1	0.013	0.013
Net Efficiency	0.35	0.7	2
Normalized blanket and shield volume	1	0.4	2.5
Central cell magnetic field	3.1 T	6.5 T	19
Total Effect on Engineering Power Density			1.2

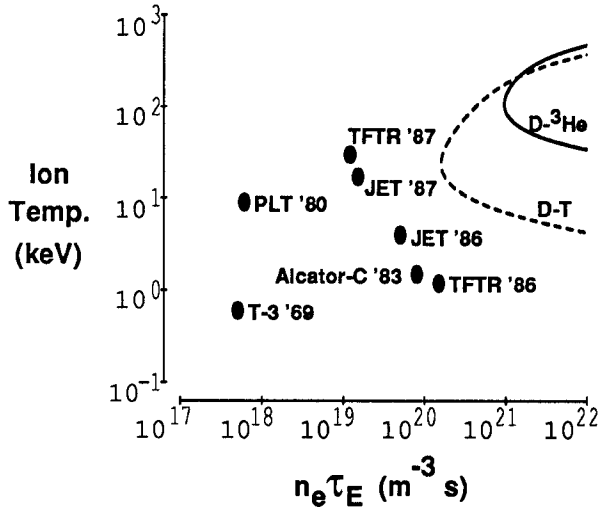

Figure 3.6. *Ignition $n_e\tau_E$ values as a function of ion temperature for the D-T and D-^{3}He fusion fuel cycles.*

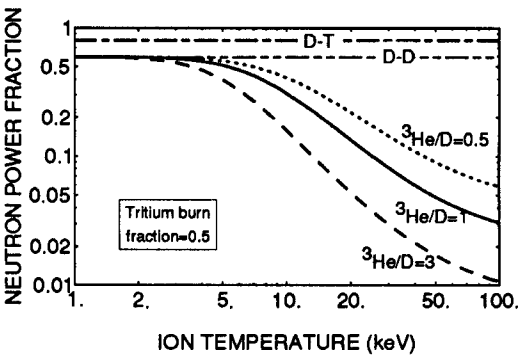

Figure 3.7. *Fraction of fusion power produced as neutrons for the D-T, D-^{3}He, and D-D fuel cycles, assuming 50% tritium burnup for D-D produced tritium.*

References for Chapter 3

[1] L.J. Wittenberg, J.F. Santarius, and G.L. Kulcinski, "Lunar Source of ^{3}He for Commercial Fusion Power," *Fusion Technol.* **10**, 167 (1986).

[2] T. Cho, M. Ichimura, M. Inutake, et al., "Scaling Studies of Thermal Barrier Potential Plasma Confinement in the Tandem Mirror GAMMA 10," in *Plasma Physics and Controlled Nuclear Fusion Research 1988*, Vol. 2, p. 501 (IAEA, Vienna, 1989).

[3] A.W. Molvik, T.A. Casper, and A.H. Futch, "Experimental Beta Limit in an Average Minimum-B Tandem Mirror," *Nucl. Fusion* **30**, 1061 (1990).

[4] J.J. Browning, R. Majeski, T. Intrator, N. Hershkowitz, and S. Meassick, "Interchange Stabilization of a Mirror Plasma Using Radio-Frequency Waves Below the Ion Cyclotron Frequency," *Phys. Fluids*, **31**, 714 (1988).

[5] N. Hershkowitz, B.A. Nelson, J.R. Ferron, R.H. Goulding, and E. Wang, "ICRF Produced Thermal Barriers in a Three-Cell Axisymmetric Tandem Mirror," *Nucl. Fusion* **28**, 1333 (1988).

[6] S. Meassick, T. Intrator, N. Hershkowitz, J. Browning, and R. Majeski, "Measurements of the Ponderomotive Force Including Sideband Mode Coupling Effects and Damping Rates," *Phys. Fluids B*, **1**, 1049 (1989).

[7] J.J. Browning, N. Hershkowitz, T. Intrator, R. Majeski, and S. Meassick, "Radio-Frequency Wave Interchange Stability Experiments Below the Ion Cyclotron Frequency," *Phys. Fluids B* **1**, 1692 (1989).

[8] S.N. Golovato, K. Brau, J. Casey, M.J. Gerver, S. Horne, et al., "Stability of Plasmas Sustained by Ion Cyclotron Wave Excitation in the Central Cell of the Tara Tandem Mirror," *Phys. Fluids B* **4**, 851 (1989).

[9] X-Z. Li, J. Kesner, and B. Lane, "MHD Stabilization of a High Beta Mirror Plasma Partially Enclosed by a Conducting Wall," *Nuclear Fusion* **27**, 101 (1987).

[10] X-Z. Li, J. Kesner, and L.L. LoDestro, "Wall Stabilized High Beta Mirror Plasma in a Rippled Magnetic Field," *Nuclear Fusion* **27**, 1259 (1987).

[11] J.A. Casey, B.G. Lane, J.H. Irby, K.L. Brau, S.N. Golovato, et al., "Experimental Studies of Divertor Stabilization in an Axisymmetric Tandem Mirror," *Phys. Fluids* **31**, 2009 (1988).

[12] R.S. Post, K. Brau, J. Casey, J. Coleman, M. Gerver, et al., "Stability Issues in the Tara Tandem Mirror Experiment," in *Plasma Physics and Controlled Nuclear Fusion Research 1988, Vol. 2*, p. 493 (IAEA, Vienna, 1989).

[13] G.D. Porter, editor, *TMX-U Final Report, Vols. 1 and 2*, Lawrence Livermore National Laboratory Report UCID-20981, Vol. 1 and 2 (1988).

[14] T.C. Simonen, H.L. Berk, T.A. Casper, and C.Y. Chen, "Low-Frequency Stability Analysis of the Tandem Mirror Experiment-Upgrade (TMX-U)," *Nucl. Fusion* **30**, 35 (1990).

[15] H.L. Berk and G.V. Roslyakov, "Anchor Stabilization of Trapped Particle Modes

in Mirror Machines," *Phys. Fluids* **30**, 478 (1987).

[16] H. Ramachandran, A.K. Sen, M.A. Lieberman, and A.J. Lichtenberg, "A Collisional Treatment of the Trapped-Particle Mode in Multiregion Mirror systems," *Phys. Fluids* **31**, 2310 (1988).

[17] W. Horton, "Drift-Mode Stability Analysis for the Tandem Mirror," *Nucl. Fusion* **20**, 321 (1980).

[18] G. Dimonte, A.W. Molvik, J. Barter, W.F. Cummins, S. Falabella, et al., "Ion Cyclotron Heating in TMX-U," *Nucl. Fusion* **27**, 1959 (1987).

[19] Y. Yasaka, M. Miyakita, S. Kimoto, H. Takeno, and R. Itatani, "Heating, Potential Formation and Barrier Pumping Using Mode Controlled ICRF in the HIEI Tandem Mirror," in *Plasma Physics and Controlled Nuclear Fusion Research 1990, Vol. 2*, p. 725 (IAEA, Vienna, 1991).

[20] J.R. Ferron, R. Goulding, B.A. Nelson, T. Intrator, En Yao, et al., "Electrostatic End Plugging Accompanied by a Central-Cell Density Increase in an Axisymmetric Tandem Mirror," *Phys. Fluids* **30**, 2855 (1987).

[21] R.A. Breun, N. Hershkowitz, P. Brooker, J. Browning, D. Brouchous, et al., "Radial Transport in the Phaedrus-B Tandem Mirror," in *Plasma Physics and Controlled Nuclear Fusion Research 1988, Vol. 2*, p. 475 (IAEA, Vienna, 1989).

[22] T. Cho, T. Kondoh, M. Hirata, A. Sakasai, N. Yamaguchi, et al., "Observation of Hot Electrons Produced by Second Harmonic Electron Cyclotron Heating in the Axisymmetric Tandem Mirror GAMMA 10," *Nucl. Fusion* **27**, 1421 (1987).

[23] T.C. Simonen and R. Horton, "The Highest Energy Confinement Measured on TMX-U," *Nucl. Fusion* **29**, 1373 (1989).

[24] G. Dimonte, "Radial Transport in a Tandem Mirror," *Phys. Rev. Lett.* **60**, 1390 (1988).

[25] K. Ishii, Y. Maeda, K. Tsumori, Y. Shimouchi, I. Katanuma, et al., "Observation of Loss Boundaries and Ion Flux Spectra of End-Loss Ions in the Tandem Mirror GAMMA 10," *Phys. Fluids B* **4**, 3823 (1992).

[26] S.K. Ho, W.M. Nevins, G.R. Smith, and G.H. Miley, "Alpha Loss-Cone Alfvén-Wave Instabilities in a Sharp-Boundary Model of a Tandem-Mirror Central Cell," *Phys. Fluids* **31**, 1656 (1988).

[27] S.K. Ho, G.R. Smith, and G.H. Miley, "Quasilinear Diffusion Modelling of the Alpha-Loss-Cone Instability in a Tandem-Mirror Reactor," *Phys. Fluids B* **1**, 2040 (1989).

[28] B.G. Logan, C.D. Henning, G.A. Carlson, R.W. Werner, D.E. Baldwin, et al., *MARS: Mirror Advanced Reactor Study*, Lawrence Livermore National Laboratory Report UCRL-53480 (1984).

[29] S. Miyoshi, T. Cho, H. Hojo, M. Ichimura, M. Inutake, et al., "Development of Tandem Mirror Experiments in GAMMA 10," in *Plasma Physics and Controlled Nuclear Fusion Research 1990, Vol. 2*, p. 539 (IAEA, Vienna, 1991).

[30] K. Yoshikawa, S. Kouda, Y. Yamamoto, and K. Maeda, "Development of a Two-Dimensional Particle Trajectory Code and Application to a Design of a Plasma Direct Energy Converter in the Fusion Engineering Facility Based on Mirror Plasma Confinement," *Fusion Technol.* **14**, 264 (1988).

[31] R.W. Moir and W.L. Barr, " 'Venetian-Blind' Direct Energy Converter for Fusion Reactors," *Nucl. Fusion* **13**, 35 (1973).

Chapter 4

Contemporary View of Tandem Mirror Fusion Power Plants

4.1 Introduction

There have been only four major power reactor studies in the past 13 years using the tandem mirror (TM) configuration: WITAMIR-I [1], MARS [2], MINIMARS [3], and Ra [4]. In addition, there have been three test facilities designed with that configuration: TASKA [5], TASKA-M [6], and TDF [7]. Only the power reactors will be addressed in this study. Table 4.1 contains the key parameters of the power reactor studies along with a column labeled Current View of D-T and D-^{3}He Reactors. The latter column contains the authors' estimate of parameters that might be used at the present time in a tandem mirror power reactor study.

4.2 Characteristics of Past D-T Commercial Reactor Studies

The key features of the D-T reactors can be compared in Table 4.1 and Figs. 4.1–4.4. In the past, it was customary to design the early reactors at high power levels ($\approx$1200 MWe) to take advantage of the economy of scale. This led to competitive reactor economics (at least relative to the tokamak). However, this also required larger capital investments and increased overall reactor lengths (Central Cell + End Plugs + Direct Converter) to 250 meters (See Fig. 4.1).

The MINIMARS [3] design was the first to investigate the smaller power levels (600 MWe) and incorporated recent physics and technology advances. The combination of these factors reduced the central cell length to less than 90 meters and the overall length to less than 140 meters.

There were also major changes in the end cell configurations in the 1980's. WITAMIR-I [1] utilized the inboard thermal barrier with yin-yang coils (see Fig. 4.2). The MARS [2] design modified that configuration by adding "C" coils (see Fig. 4.2) and introduced ion bounce frequency drift pumping of the barrier region. When the MINIMARS [3] project was initiated, a single cell thermal barrier approach was used with an octupole plug. The barrier pumping was accomplished by ponderomotive drift pumping. The MINIMARS design also included a gridless direct converter configuration which could better accommodate the spreading of the ion energy in the central cell. This approach was able to lower the hot electron temperatures in the barrier from $\approx$800 keV in MARS to $<$300 keV in MINIMARS. This concept reduced the power level of ECRF injected in the end cell by a factor of $\approx$2, albeit at a frequency of approximately 2 times higher (110 GHz in MINIMARS vs. 60 GHz in MARS).

The technology requirements of the central cell were modest in all three reactor designs. Common features included (see Fig. 4.4 and Table 4.1):

Table 4.1- Summary of Past Tandem Mirror Power Reactors

Parameter	Units	WITAMIR	Mars	MiniMars	Ra	Current View DT Reactor	Current View D3He Reactor
			Overall Reactor				
Year Published		1980	1984	1986	1987	1992	1992
Fuel		DT	DT	DT	D3He, 3:1	DT	D3He 1:1
Fusion Power	MW(th)	3000	2600	1290	1227	1290	990
Net Electric Power	MW(e)	1530	1200	600	600	600	600
Net Efficiency	%	39	34	35	49	35	53
Reactor Length (CC+EP)	m	207	194	104	109	98	90
Overall Length (CC+EP+DC)	m	250	220	138	158	132	140
			Central Cell				
CC Length	m	165	131	88	100	88	81
ID Plasma Chamber	m	1.94					
Max. CC Magnetic Field	T	3.6	4.7	3.08	6.5	3.08	6.5
Ion Density	10^14/cm3	1.51	3.3	3.96	1.26	3.96	3
Ion Energy	keV	32.5	28	24.7	83	25	100
n Wall Loading	MW/m2	2.4	4.3	3.3	0.05	3.3	0.1
<beta>	%	40	28	60	73	60	73
Fueling		Beams/Pellet Injection	Pellet Injection	Laser Propelled Pellets	Undetermined	Compact Toroid	Compact Toroid
			End Cell				
Type		Inboard Thermal Barrier with Yin Yang Coils	Inboard Thermal Barrier with Yin Yang & "C" Coils	Single Cell Thermal Barrier With Octupole Plug	Axisymetric With RF Stabilization	Axisymmetric	Axisymmetric
Maximum Choke Magnet Field	T	14.1	24	24	24 (16+8)	24	24
<Ion Energy>	keV	905	690 (anchor)	≈500	880	≈500	880
<Hot Electron Eng. in Barrier>	keV	270	820	297	434	297	434
<Warm Electron Temp. in Plug>	keV	123	123	277	336	277	336
			Central Cell Materials				
Structural		HT-9	HT-9	HT-9	Stainless Steel	HT-9	Low Activation Stainless Steel
Maximum Temp. of Structure	°C	530	550	525	300	525	550
Neutron Damage	dpa/FPY	40.5	60	46	0.5	46	1
Helium Production	appm/FPY	281	500	380	<3	380	<6
Neutron Multiplier		None (Pb)	None (Pb)	Be, Pb	None	None(Pb)	None
n Energy Multiplication		1.37	1.362	1.46	2.4	1.36	2.4
			Coolant				
Type		Li17Pb83	Li17Pb83	Helium @ 8MPa	water	Li17Pb83	Pb
T(in)/T(out)	°C	330/500	350/500	275/575	218/300	350/500	350/500
			Breeder				
Type		Li17Pb83	Li17Pb83	Li17Pb83	None	Li17Pb83	None
Tritium Breeding Ratio		1.07	1.15	1.067	None	1.07	None
Blanket T2 Inventory	g	101 (8)	7	6	None	6	None
			End Cell Heating				
Hot Ion NBI Beams	MWe/keV	37/500	14/475	12/412	8/2000	12/412	8/2000
Anchor ICRF	MWe/MHz	-	25/55	-	-	-	-
RF Stabilizing RF	MWe/MHz	-	-	-	38/196	-	38/196
Mantle ECRF	MWe/GHz	-	-	33/110	-	-	-
Warm-Electron Plug ECRF	MWe/GHz	33/112	9/71	4/70	11/195	4/70	11/195
Hot-Electron Barrier ECRF	MWe/GHz	67/40	110/60	23/110	25/13	23/110	25/13
			Barrier Pumping				
Mechanism		Neutral Beams	Ion bounce frequency drift pumping	Ponderomotive drift pumping	Pondero-motive drift pumping	Ponderomotive drift pumping	Ponderomotive drift pumping
Low Energy NBI	MWe/keV	12/10	-	-	-	-	-
High Energy NBI	MWe/keV	85/190	-	-	-	-	-
RF system	MWe/MHz	-	20/0.05-.6	50/46	25/144	50/46	25/144
			Direct Converter				
Type		Venetian Blind	Venetian Blind	Gridless	Venetian Blind	Gridless	Venetian Blind
Net Electric Power From Direct Converter	MW(e)	302	292	82	400	82	375
Coolant		H2O	H2O	H2O	H2O	H2O	H2O
			Economics (in Year of Publication)				
Unit Capital Costs	$/kWe	2130	2437	2740	2283	2600 (1986)	1850 (1987)
Cost of Electricity	mills/kWh	36	46	41	34 + fuel	39 (1986)	27 + Fuel (1987)

Tandem Mirror Power Reactor Overall Configuration

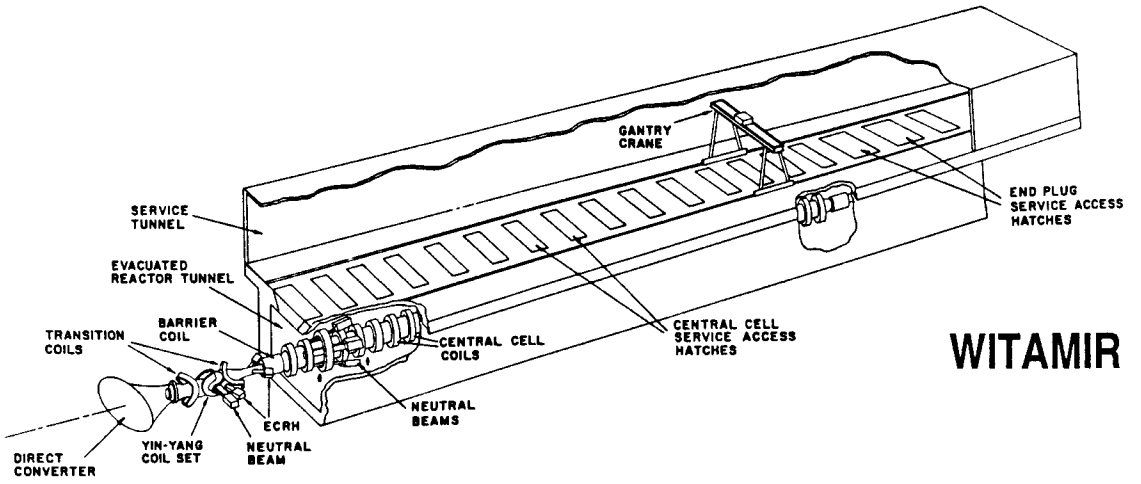

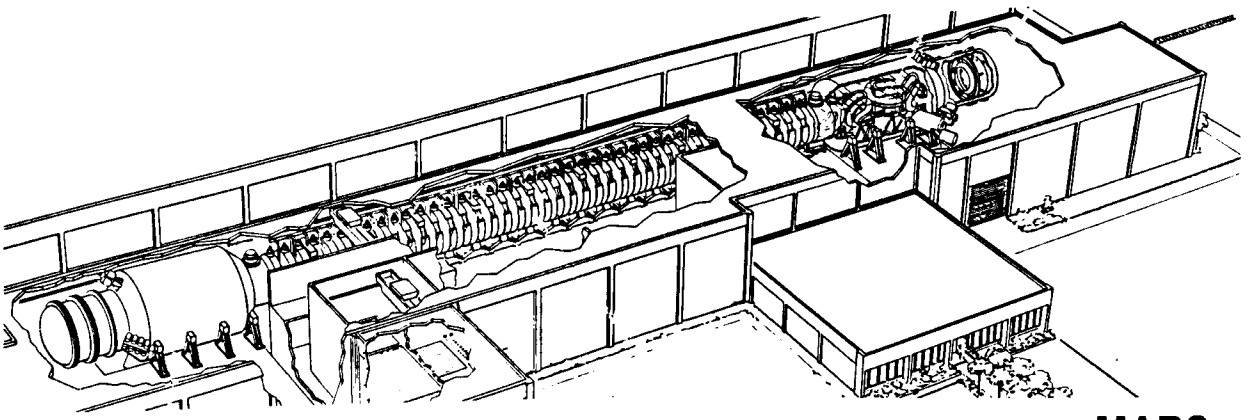

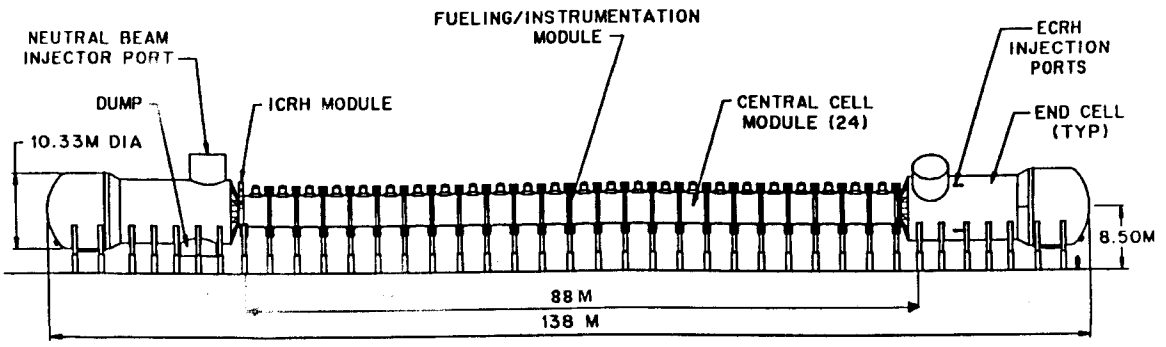

Figure 4.1

Tandem Mirror Power Reactor End Cells

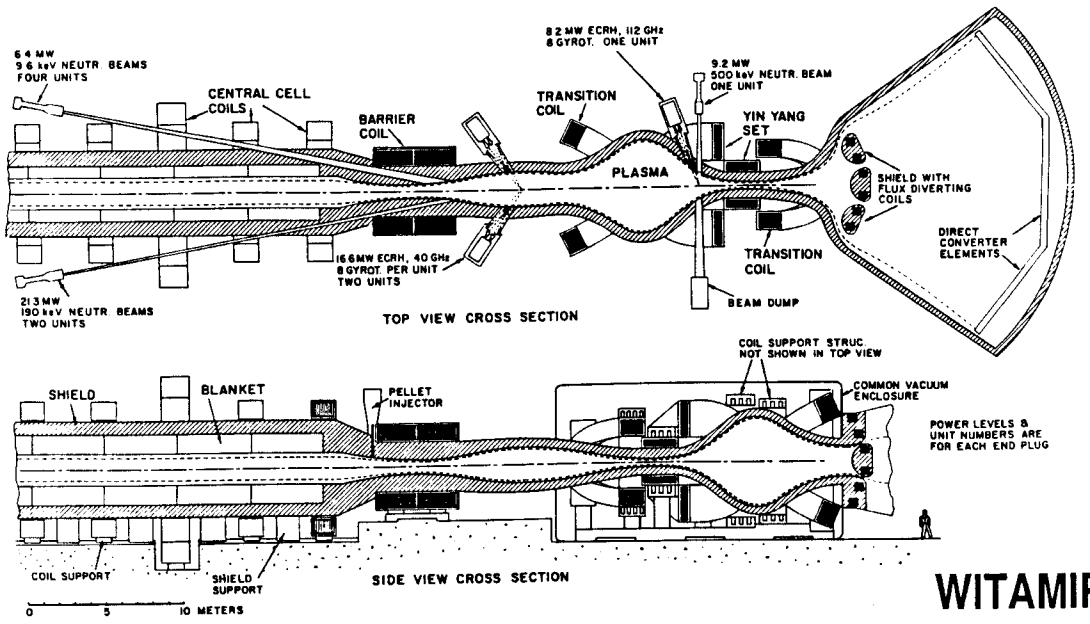

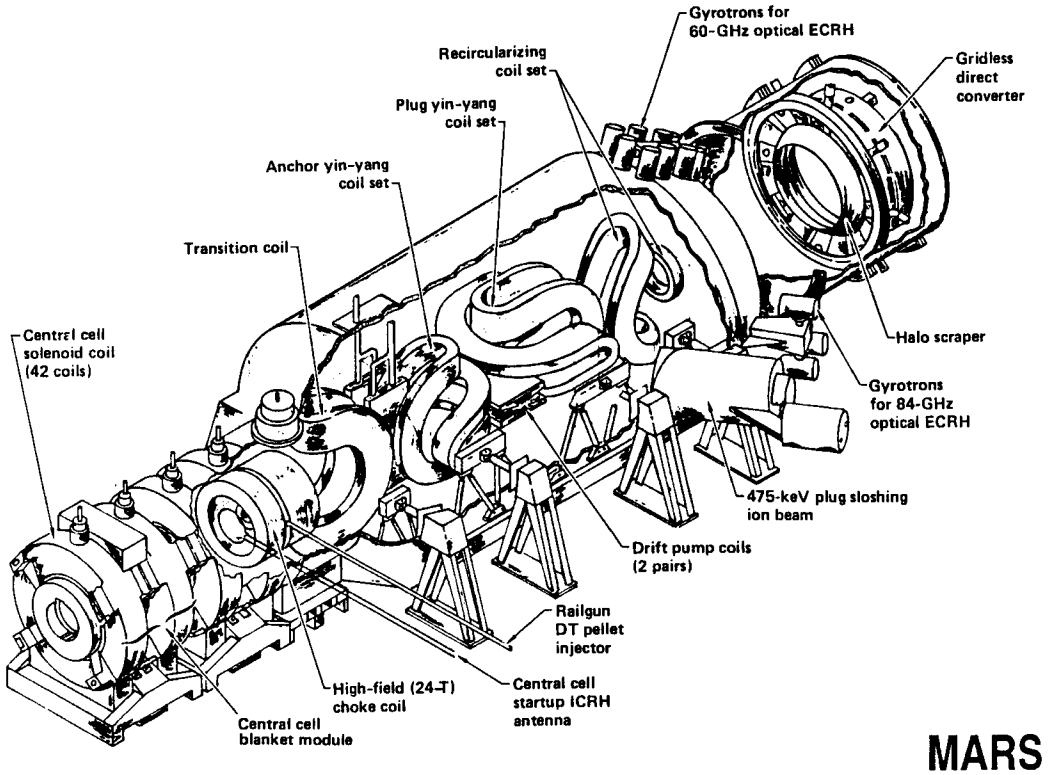

Figure 4.2

MINIMARS Tandem Mirror Power Reactor End Cell

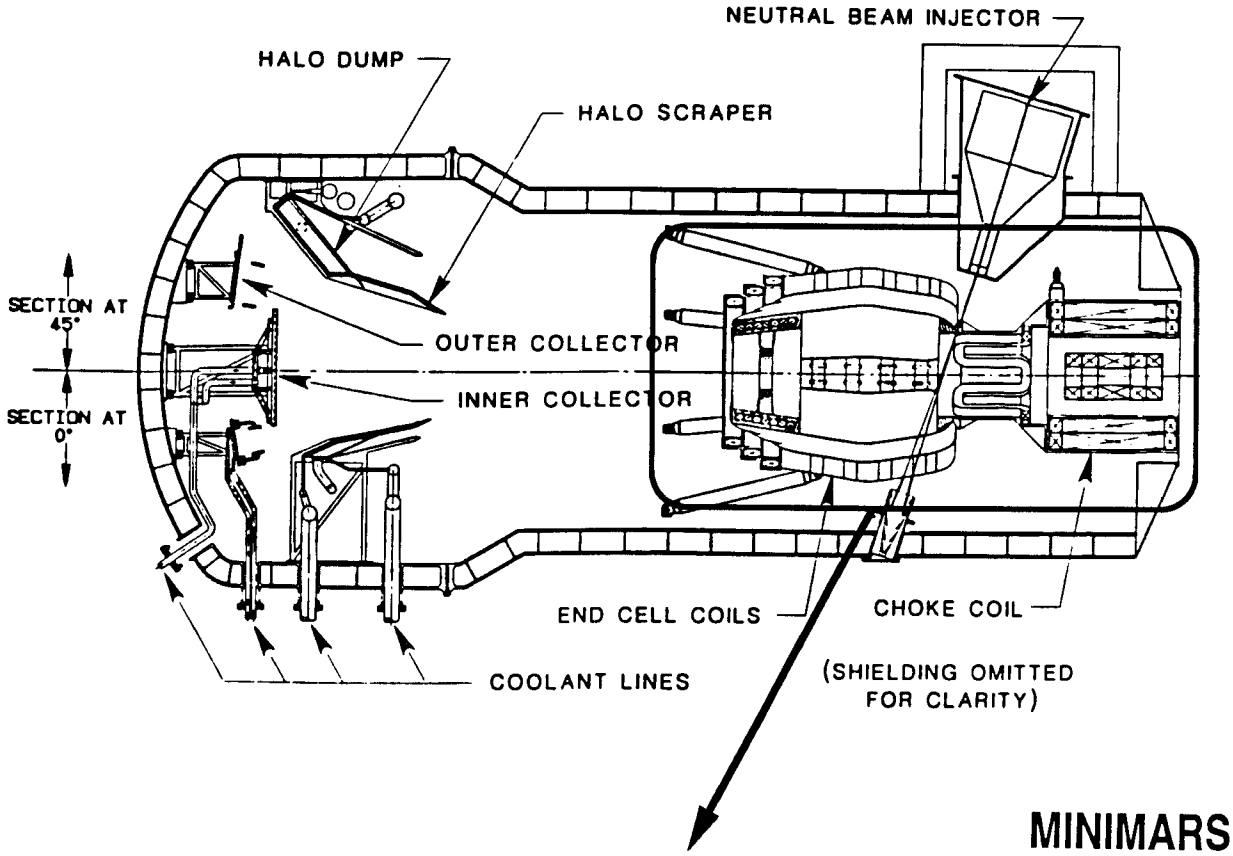

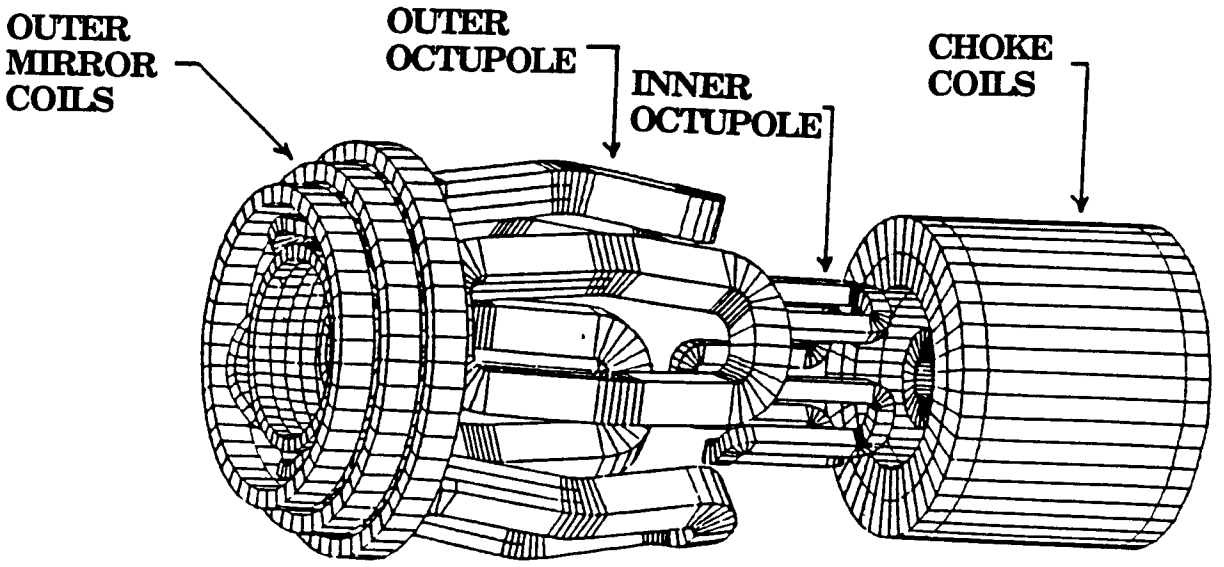

Figure 4.3

Tandem Mirror Power Reactor Central Cells

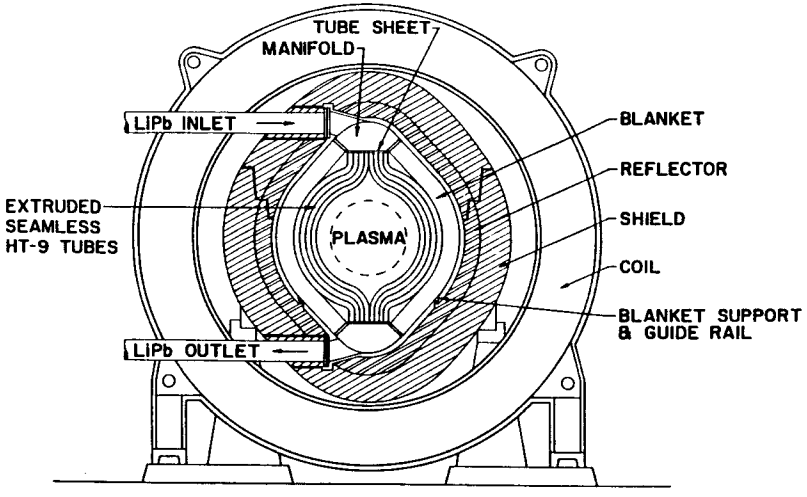

WITAMIR

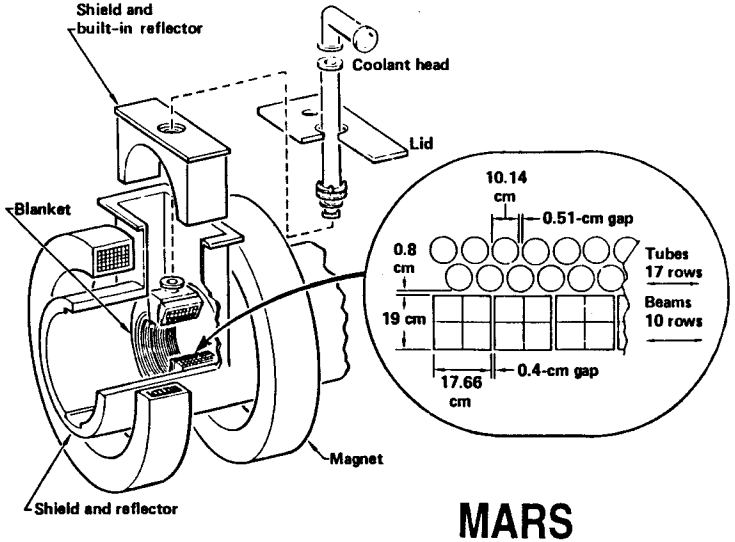

MARS

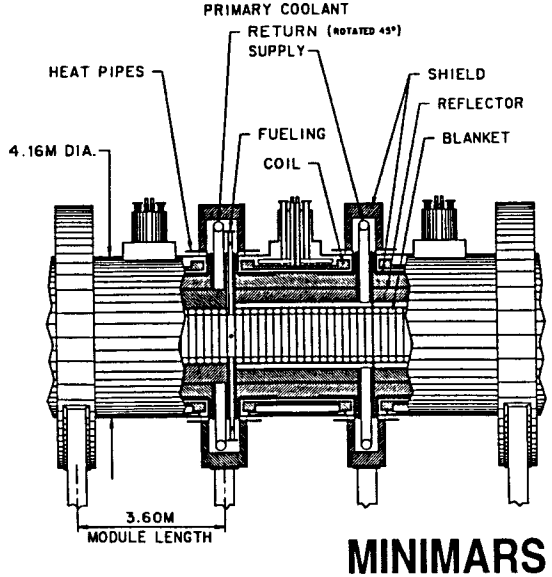

MINIMARS

Figure 4.4

- Modest central cell solenoidal coil fields of 3–5 tesla.
- Fueling of the plasma by pellets containing D and T.
- Use of economical and highly radiation damage resistant ferritic steels, HT-9.
- A coolant-breeder ($Li_{17}Pb_{83}$) that could operate at high temperatures (≈500°C) with a high neutron energy multiplication (≈1.4) and generate an adequate tritium breeding ratio (≈1.1).
- Peak neutron wall loadings of ≈2 to 4 MW/m^2.
- Low tritium inventories in the breeder material (≈6 to 8 grams)
- Relatively easy maintenance (compared to toroidal systems) associated with the cylindrical geometry (see Fig. 4.4).

The simple geometry of the central cell, where most of the neutrons are produced, allowed the designers to develop maintenance and repair schemes which are probably the most credible of all the nearly 50 power reactor studies performed in the 70's, 80's and 90's.

4.3 Implications of Reactor Studies for Heating and Fueling Technology

4.3.1 Heating Technology

Tandem mirror reactors utilize neutral beams for injection into the end plugs to produce the mirror-confined ions, electron cyclotron heating to produce hot electrons in the end plugs and to produce thermal barriers, and ion cyclotron heating to heat the central cell ions during startup. The neutral beam requirements identified in tandem mirror reactor studies are relatively modest in power but require high energy by present standards for fusion experimental devices. The MARS [31] study set the neutral beams at 4.4 MW per end plug with an energy of 475 keV; the injected species is D_0. This beam energy requires negative ion technology, a field which has advanced considerably in the last few years due to the Strategic Defense Initiative. This is also a modest neutral beam compared with the requirements for neutral beam current drive in ITER (75 MW at 1.3 MeV [8]).

The ECRH technology requirements identified in the MARS study are for about 80 MW with frequencies in the range 70–110 GHz. This should be compared with the ITER [8] requirements for 20 MW at 140 GHz for plasma heating and current profile control. The proposed sources for the MARS study are gyrotrons and free electron masers. Steady-state operation and high efficiency (about 80%) to keep the recirculating power low are required.

The tandem mirror reactor studies use ICRF heating to heat the central cell during startup. The needs are modest, about 10 MW at frequencies in the range 25–70 MHz. This is the typical frequency range (20–100 MHz) for ICRF heating in tokamaks and the power is less than that in JET (18 MW).

4.3.2 Fueling Technology

Fueling of fusion grade plasmas is a generic problem for long-pulse or steady-state reactors. The plug region of a tandem mirror is naturally fueled by the neutral beams producing the hot ion population. Fueling is required in the central cell to replace the losses by escape out the ends, by radial transport, and by fusion burnup. Tandem mirror experiments (e.g. TMX-U) used gas puffing into the central cell to maintain the plasma density. This is not an option for reactors since the penetration of gas is very poor in large, high density plasmas. The usual assumption in tandem mirror reactors is that end-loss

dominates over radial loss; furthermore, there is no reason to believe there is a pinch effect to take plasma from the edge to the axis of the central cell. Consequently, penetration of the fueling source all the way to the axis is believed to be required. Fueling of the central cell using neutral beams alone is also not an option since the energy required for penetration combined with the necessary injection current implies an enormous power input to the central cell; this upsets the power balance on the central cell and of the whole system. In addition, it produces ions with an average energy higher than that which maximizes the fusion reaction rate for a given plasma beta. The options for fueling that have been identified are pellet injection and plasma injection.

Pellet injection in tandem mirror reactors is similar to pellet injection in tokamak reactors. The MARS reactor study [2] analyzed pellet injection for fueling and concluded that an injection velocity of about 25–30 km/s was needed for a pellet diameter of 4 mm. The required repetition rate was 6 pellet/s. In order to minimize the required injection velocity, the pellets were injected near the throat of the choke coils forming the ends of the central cell. The plasma radius there is about one-half the radius in the main part of the central cell. For MARS a rail-gun pellet accelerator with a centrifugal pre-injector was proposed. The MINIMARS reactor study [3] had similar requirements for fueling and also considered pellet injection; they proposed, however, a laser-ablation acceleration scheme. Both of these pellet acceleration schemes require considerable development before they can be considered to be practical.

Plasma injection is receiving some interest for injection into tokamaks since the formation of compact toroid plasmas and their subsequent acceleration has been achieved in the RACE experiment at LLNL. Compact toroid injection can easily produce the injection velocity necessary to penetrate to the plasma center, although this concept has not received much attention in the current experimental program for tokamaks. Critical issues for compact toroid injection are achieving the required repetition rate and being able to insure that the plasma being injected is sufficiently clean. Present compact toroid plasmas are formed in a Marshall gun which has electrodes in contact with the plasma, so they are notorious for producing dirty plasmas. Little attention has been given to plasma formation using electrode-less techniques so the ultimate potential for producing a clean plasma for injection is not known.

4.4 Performance Characteristics of an Advanced Fuel Tandem Mirror Power Reactor

In 1987, the advantages and disadvantages of using a D-^{3}He fuel cycle in a tandem mirror configuration were examined [4]. Because most of the energy from this reaction is in the form of charged particles, a strong emphasis was placed on the use of direct converters. A power level of 600 MWe was chosen so as to be comparable to the most recent D-T tandem mirror power reactor study, MINIMARS [3]. One of the first non-intuitive observations one makes from Table 4.1 is that even though the overall efficiency of Ra is 49% compared to 35% in MINIMARS, the fusion powers are approximately the same in both reactors. The explanation lies in the fact that in D-T systems, the energy deposited by neutrons in the blanket is multiplied by a factor of $\approx$1.4. In a D-^{3}He system there are few neutrons and the increased electrical conversion efficiency basically balances the "loss" in total energy production from the neutrons.

A few of the features on Ra which differ from the D-T designs include:

- Axisymmetric end cells with RF stabilization.
- Use of low activation austenitic alloys.

- Very low neutron wall loading (≈0.05 MW/m^2).
- Permanent first wall life due to neutron damage.
- No tritium breeding.
- Water cooling of the blanket/shield at modest temperatures, 300°C.
- Use of 2 MeV NBI's for the hot ions.
- 195 GHz ECRF power to the warm electrons in the plugs.
- A large fraction of the gross electrical power from the direct converter (≈400 MWe).
- One of the lowest capital costs of a fusion power plant ever designed (<2300 $/kWe).

The level of detail on the Ra design was much smaller than that in the previous D-T tandem mirror reactor studies because of the premature shutdown of the mirror program.

4.5 Current View of D-T Tandem Mirror Reactors

If the mirror program were to be revitalized in 1992, what would designers do differently than before? In an attempt to answer that question, possible reactor configurations for both fuel cycles are shown in Table 4.1. The reader should recognize that while every attempt was made to make the parameters self consistent, a full-fledged reactor design study would be necessary to assure complete self consistency.

It is felt that only a few improvements that could be made in the D-T MINIMARS reactor concept and these are listed below:

- Use of compact toroid fueling
- Axisymmetric end cells
- Optimize the HT-9/$Li_{17}Pb_{83}$ blanket design and remove Be.

The use of an axisymmetric end plug would result in a major simplification of the coil design, construction, shielding, and maintenance. This concept alone would place the tandem mirror far ahead of toroidal systems when it comes to engineering credibility.

Such changes would have a relatively small effect on the COE and on the safety of the reactor. This is not to say that little improvement is possible, only that the past D-T designs were rather robust. Given that the plasma issues can be satisfactorily resolved, the MINIMARS reactor was very attractive in its own right.

4.6 Current View of D-^{3}He Tandem Mirror Reactors

One of the first changes one might implement in the D-^{3}He tandem mirror reactor would be to adjust the ^{3}He/D ratio from 3:1 in Ra to 1:1 in a current reactor. This would increase the power density enough so that more fusion power in charged particles could be extracted to the direct converter. The end result would be a higher overall efficiency (53 vs. 49%), a lower fusion power required (990 vs. 1230 MW), and a shorter central cell (81 vs. 100 m). On the negative side, the neutron wall loading would double from the low value of 0.05 to ≈0.1 MW/m^2.

An important solution to the fuel-injection problem would be the use of a compact-toroid injection system. This would resolve one of the key uncertainties of the Ra design.

Another improvement in a D-^{3}He tandem mirror design would be to abandon the concept of low temperature structure and maximize the thermal conversion efficiency by using a Pb coolant instead of water. This makes more sense in a low neutron wall loading scenario than in a high wall loading situation as in MINIMARS because metals are notoriously brittle after high

temperature exposure to neutrons. The cumulative fluence of ≈3 MW-y/m^2 on the first wall over the life of the reactor should still allow those components to last for the entire reactor lifetime.

The effect of the three changes above might make a ≈20% impact on the COE and/or the capital cost making a current D-^{3}He tandem mirror even more attractive now than 5 years ago.

4.7 Conclusions

The overall conclusion of this analysis is that the engineering and technology of past tandem mirror power reactor designs was sufficiently conservative and robust that the key emphasis of any revived mirror program has to focus on the solution of the plasma physics problems, not on the technology challenges. Said in another way, once the physics problems are solved, the path to a commercial tandem mirror reactor should be much easier than for a toroidal configuration.

References for Chapter 4

[1] B. Badger, K. Audenaerde, J.B. Beyer, D. Braun, J.D. Callen, et al., "WITAMIR-I: A University of Wisconsin Tandem Mirror Reactor Design," University of Wisconsin Report UWFDM-400, September 1980.

[2] B.G. Logan, C.D. Henning, G.A. Carlson, R.W. Werner, D.E. Baldwin, et al., "MARS: Mirror Advanced Reactor Study," Lawrence Livermore National Laboratory Report UCRL-53480, Volumes 1-A, 1-B and 2, 1984.

[3] J.D. Lee, Technical Editor, "MINIMARS Conceptual Design: Final Report," Lawrence Livermore National Laboratory Report, UCID-20773, Volumes I and II, September 1986.

[4] J.F. Santarius, H.M. Attaya, M.L. Corradini, L.A. El-Guebaly, G.A. Emmert, et al., "Ra: A High Efficiency, D-^{3}He, Tandem Mirror Fusion Reactor," UWFDM-741, also 12th Symposium on Fusion Engineering, p. 752, Monterey, CA, October 1987.

[5] B. Badger, W. Heinz et al., "TASKA-Tandem Spiegelmachine Karlsruhe, A Tandem Mirror Fusion Engineering Facillity," University of Wisconsin Report, UWFDM-500, Kernforschungszentrum Karlsruhe Report, KfK-3311, March 1982.

[6] B. Badger, W. Heinz et al., "TASKA-M, A Low Cost, Near Term Mirror Device for Fusion Technology Testing," University of Wisconsin Report UWFDM-600, Kernforschungszentrum Karlsruhe KfK-3680, December 1983.

[7] K.I. Thomassen, J.N. Doggett, B.G. Logan, et al., "A Tandem Mirror Technology Demonstration Facility," Lawrence Livermore National Laboratory Report UCID-19328, October 1983.

[8] V.V. Parail, N. Fujisawa, H. Hopman, et al., "ITER Current Drive and Heating System," ITER Documentation Series No. 32 (International Atomic Energy Agency, Vienna, 1991).

Chapter 5

Critical Issues for the Advancement of the Tandem Mirror as a Reactor

5.1 Introduction

The state of tandem mirror research has not advanced as far as that of the tokamak, because the tandem mirror is a more recent invention and there have been only a few tandem mirrors compared with the more numerous and much larger tokamak experiments. The tandem mirror approach to fusion was invented in 1976 and terminated in 1986, at least in the U.S.; there are only about 40 machine-years of experience accumulated with tandem mirrors, including non-thermal barrier tandem mirrors. The largest tandem mirror, MFTF-B, was canceled after construction of the magnet system and the vacuum chamber, but before it could operate.

The present experimental data base for tandem mirrors, despite having made considerable progress in the 10 years in which there was a substantial program in the U.S., is currently inadequate for building a reactor and needs to be expanded. Shown in Table 5.1 [1]–[8] are the parameters achieved in experiments and the approximate requirements for a reactor. If the tandem mirror is to be considered as a reactor concept, a number of critical physics questions require further exploration. Among the various questions one might consider, we propose the following as needing further investigation and being important to the success of the tandem mirror as a reactor concept.

5.2 Loss of End Plugging and Thermal Barrier Physics

The TMX-U tandem mirror experienced a loss of central cell plugging when the central cell density was higher than about 3×10^{18} m^{-3} [2, 9]. The cause for this was unknown, but it prevented the machine from reaching its design goal. GAMMA-10 has not reported experiencing this loss of plugging, but their operating range for the central cell density is from 10^{18} m^{-3} to about 10^{19} m^{-3} [1] at the highest. Phaedrus and Tara also operated only in the low central cell density region. Successful operation with a thermal barrier at central cell densities of the order of 10^{20} m^{-3} is required in order to demonstrate the reactor potential of the tandem mirror. It is also important to understand the reason for this loss of plugging so that the phenomenon can be avoided in future experiments.

5.3 Achieving Reactor Relevant Parameters in a Microstable Plasma

The present experimental database (see Table 5.1) is restricted to low densities and temperatures compared with those needed for a reactor. While the present experiments with thermal barrier tandem mirrors have shown that microinstabilities can be largely avoided through

Table 5.1. *Tandem mirror parameters achieved and required.*

Parameter	Best Achieved	Reactor [8]
Central Cell		
Density (m^{-3})	1.1×10^{19} [1]	4×10^{20}
Ion temperature (keV), $T_{i\perp}$	5.6 [1]	25
Ion temperature (keV), $T_{i\|\|}$	0.3 [6]	25
Electron temperature (keV), T_{ec}	0.28 [2]	20
Beta (%)	13 [3]	60
$n\tau_{p\|\|}$ (m^{-3} s)	1×10^{19} [1]	1×10^{21}
End Plug or Anchor		
Plug-to-central cell density ratio	0.4 [1]	–
Beta (%)	15 [4]	25
Ion confining potential (kV), ϕ_c	2.0 [5]	148
ϕ_c/T_{ic}	5.5 [6]	7.4
Thermal Barrier		
Barrier potential (kV)	1.1 [1]	126
Hot electron energy (keV)	50 [4] -100 [7]	297

careful control of parameters, this needs to be demonstrated at reactor-relevant conditions. The usual consequence of microinstabilities is that confinement is rapidly degraded. Hence, microinstabilities must be avoided at all cost. In addition to the microinstabilities driven by loss-cones, anisotropy, and density gradients, there is also the potential for microinstabilities to be driven by the fusion products in a reacting plasma.

5.4 Purely Axisymmetric Operation with MHD Stability

The use of quadrupole or higher order minimum-B end cells poses severe problems for a tandem mirror reactor. The complexity and cost of yin-yang magnets is an important factor determining the engineering and economic viability of the tandem mirror concept. The lack of axisymmetry inherent in the quadrupole magnets is the primary cause of the rapid radial transport seen in TMX-U. GAMMA-10 placed the quadrupole magnets inboard of the end-cell and took advantage of a canceling of the non-axisymmetric fields when the ions pass through the entire quadrupole magnets before being reflected by the confining potential in the end-cells. As a result, enhanced radial transport was small in GAMMA-10. However, this configuration is not desirable for a reactor, because it requires high-field, heavily shielded quadrupole magnets due to the high pressure of the central cell plasma streaming through the quadrupole anchor. The tandem mirror concept would be considerably improved if operation with purely axisymmetric magnets proves to be feasible.

There is hope that axisymmetric operation may be possible. Phaedrus operated successfully using RF stabilization with purely axisymmetric fields and achieved a central cell beta of 13%. Subsequently, RF stabilization was also seen in Tara. This is a very intriguing result and, if ex-

trapolatable to a reactor, would lead to considerable simplification of the tandem mirror concept from an engineering viewpoint. Considerable theoretical attention has been given to RF stabilization, but experimental demonstration of RF stabilization in denser and hotter plasmas is required. Furthermore, RF stabilization would need to be effective at central cell betas of about 50% to 60% in order to be useful in a reactor and the RF power required should be sufficiently low so that the recirculating power fraction is not excessive.

There are other possibilities for axisymmetric operation which do not require RF power. These include the magnetic divertor concept, tested on Tara, and wall stabilization. These concepts are discussed in more detail in Sec. 2.2.3.

5.5 Thermal Barrier Pumping

The TMX-U and GAMMA-10 tandem mirrors used neutral beams to pump out ions that became collisionally trapped in the thermal barriers; this is straightforward from a physics viewpoint since it depends on atomic collisions and geometry, but is expensive in terms of the required beam power. There have been several proposals for pumping the thermal barrier using guiding-center drifts [10] or waves to enhance the radial loss of barrier-trapped ions. These concepts are discussed further in Sec. 2.4.4. Barrier pumping by guiding center drifts can have the effect of introducing non-axisymmetry in the central cell potential and thereby cause azimuthal electric fields which enhance the radial transport of the central cell plasma [11].

Using waves or stochastic fields to induce radial transport in the thermal barrier and thereby remove trapped ions is an intriguing concept requiring further exploration to see if it is feasible. It also has the advantage of being consistent with axisymmetry, but has the possible disadvantage that it may also enhance the radial transport of passing ions and thereby enhance central cell loss. Clearly, further investigation is needed to determine the practicality of these ideas, but their successful implementation will greatly reduce the amount of recirculating power in tandem mirror reactors.

5.6 Impurity Control

The thermal barrier is an electrostatic well and thus is a natural accumulation point for impurity ions. Impurity accumulation needs to be avoided; this will probably require a plasma halo which shields the central cell and thermal barrier plasma from wall-originated impurities in much the same manner as the scrape-off layer plasma in tokamaks. The plasma halo will also shield the plasma from the neutral gas and associated charge exchange losses. In addition, the barrier pumping scheme needs to be able to remove impurities, especially the fusion product ash. These concepts require experimental demonstration in a steady-state plasma.

5.7 Enhanced Central Cell Confining Potentials

End cell potentials greater than that expected from the density ratio and the Boltzmann relation have been achieved in Phaedrus [12] when RF power is used in the end plugs. This result has been interpreted as due to the pumping of electrons by the parallel component of the wave electric field. This suggests that RF waves in the ion cyclotron frequency range can be used to enhance the ion confining potential. While not a critical issue, this development offers a means for increasing the ion confining potentials and thereby reducing the demand on the thermal barrier and high power ECH in the plug.

5.8 Next Steps in an Experimental Program

In order to advance the tandem mirror as a reactor concept, an experimental program which addresses the critical issues discussed in Sec. 5.2–5.7 is required. Reasonable next steps in such an experimental program would be to:

1. Establish successful operation in an experiment the size of GAMMA-10 but based on axisymmetric end cells and achieve MHD stable operation at a central cell beta of about 25%.
2. Develop alternative thermal barrier pumping concepts (see Sec. 2.4.4 and 5.5) in this device.
3. Build an experiment of about the size and magnetic field strength of MFTF-B, but with axisymmetric end cells. Reasonable goals for the central cell parameters would be a density of 3×10^{19} m^{-3}, an ion temperature of 15 keV, an electron temperature of 6 keV, and an $n\tau_p$ of 6×10^{19} m^{-3} s. These parameters are essentially the goals of the (cancelled) MFTF-B experiment.

This set of parameters, if achieved, would produce a plasma roughly equivalent to that achieved to date in tokamaks and would allow researchers to investigate

- microstability
- MHD stability
- axisymmetric end cells
- thermal barrier physics
- thermal barrier pumping
- impurity control

in reactor-relevant plasma conditions.

Successfully achieving these goals would essentially establish the physics basis for proceeding with the tandem mirror as a reactor concept and thereby allow the fusion program to realize the technological advantages of the tandem mirror as a reactor concept.

References for Chapter 5

[1] S. Miyoshi, T. Cho, H. Hojo, et al., "Development of Tandem Mirror Experiments in GAMMA 10," in *Plasma Physics and Controlled Nuclear Fusion Research 1990*, Vol. 2, p. 539 (IAEA, Vienna, 1991).

[2] T.C. Simonen S.L. Allen, D.E. Baldwin, et al., "TMX-U Tandem Mirror Thermal Barrier Experiments," in *Plasma Physics and Controlled Nuclear Fusion Research 1986*, Vol. 2, p. 231 (IAEA, Vienna, 1987).

[3] R.A. Breun, P. Brooker, D. Brochous, et al., "Stabilization of MHD Modes in an Axisymmetric Magnetic Mirror by Applied RF Waves and Initial Results with Phaedrus-B," in *Plasma Physics and Controlled Nuclear Fusion Research 1986*, Vol. 2, p. 263 (IAEA, Vienna, 1987).

[4] R.S. Post, M. Gerver, J. Kesner, et al., "Tara and Constance B Mirror Confinement Experiments and Theory," in *Plasma Physics and Controlled Nuclear Fusion Research 1984*, Vol. 2, p. 285 (IAEA, Vienna, 1985).

[5] T. Tamano, T. Cho, M. Hirata, et al., "Confinement Studies in the Tandem Mirror GAMMA 10," *in Plasma Physics and Controlled Nuclear Fusion Research 1992*, (to be published by IAEA, Vienna).

[6] T. Cho, M. Ichimura, M. Inutake, et al., "Scaling Studies of Thermal Barrier Potential Plasma Confinement in the Tandem Mirror GAMMA 10," in *Plasma Physics and Controlled Nuclear Fusion Research 1988*, Vol. 2, p. 501 (IAEA, Vienna, 1989).

[7] R.S. Post, K. Brau, J. Casey, et al., "Stability Issues in the Tara Tandem Mirror Experiment," in *Plasma Physics and Controlled Nuclear Fusion Research 1988*, Vol. 2, p. 493 (IAEA, Vienna, 1989).

[8] J.D. Lee, Technical Editor, MINIMARS Conceptual Design: Final Report, Lawrence Livermore National Laboratory Report UCID-20773, Vols. I and II (1986).

[9] R.F. Post, "The Magnetic Mirror Approach to Fusion," *Nuclear Fusion*, **27**, 1579 (1987).

[10] J. Kesner, *Comments on Plasma Physics and Controlled Fusion*, **5**, 123 (1979).

[11] D.G. Braun and G.A. Emmert, "Drift Orbit Pumping in Thermal Barriers," *Bull. Amer. Phys. Soc.*, **25**, 980 (1980).

[12] R.A. Breun, N. Hershkowitz, P. Brooker, et al., "Radial Transport in the Phaedrus-B Tandem Mirror," in *Plasma Physics and Controlled Nuclear Fusion Research 1988*, Vol. 2, p. 475 (IAEA, Vienna, 1989).

Chapter 6

Summary and Conclusions

The state of the mirror program prior to 1986 was characterized by a strong effort in the United States; the program at Lawrence Livermore National Laboratory was aggressive and was backed by substantial university programs at Wisconsin and MIT. In addition, there were substantial programs in Japan and in the USSR. There was no program in Europe, however. The achieved experimental results for tandem mirror research were considerably behind those from toroidal machines, especially tokamaks, but this should be understood in the context that the worldwide investment in tokamaks was a factor of 10-20 larger than that for mirrors and related concepts. Because of budgetary pressures and because tokamaks were able to produce plasmas closer to those needed for an ignition experiment, the decision was made in the U.S. to terminate the mirror line of fusion research in 1986. The effect was felt initially at Livermore where MFTF-B was mothballed before operation and TMX-U was canceled. The university programs continued for a few years but were eventually phased out. The programs in Japan and the USSR continued, although the USSR program was hampered by technical difficulties with the equipment, so their contribution to tandem mirror research has been largely with respect to theory and not experiment.

Despite the decision to terminate the mirror line of research, considerable progress had been made in tandem mirror research by 1986. The primary achievements were:

- the demonstration of the tandem mirror concept of electrostatic confinement of the central cell ions in TMX,
- the reduction of the particle end-loss from the central cell by at least a couple of orders of magnitude compared with that due to simple mirror loss,
- the establishment of thermal barriers in TMX-U, GAMMA-10, and Phaedrus,
- the demonstration that tandem mirrors can be made stable against the microinstabilities that degrade mirror confinement,
- the establishment of MHD stable plasmas using the concept of pressure weighting of regions of good magnetic curvature.

It must be recognized, however, that TMX-U did not meet the goals that had been established for the experiment when it was authorized. The thermal barrier was obtained only at low density (less than 3×10^{18} m^{-3}, which is about a factor of three below the goal). In addition, the electron temperature in the central cell in TMX-U was no higher than that in TMX (about 280 eV). This failure to meet the promises made for TMX-U may have been another factor in the decision to terminate the mirror program in the U.S.

Since 1986, the mirror program has continued to advance, although at a slower rate. The GAMMA-10 experiment in Japan has achieved improvements in the central cell density, the

electrostatic potential confining the central cell ions, and the potential in the thermal barrier which thermally isolates the plug electrons from the central cell electrons. There has also been experimental corroboration of much of the theoretical basis for the tandem mirror, especially microstability, MHD stabilization, scaling of end-loss, and the establishment of electrostatic potentials. In addition, newer concepts for end cells have emerged from experiment and theory. These include the possibility of axisymmetric end cells stabilized by RF waves or magnetic divertor configurations and the use of RF waves to enhance electrostatic potentials and pump thermal barriers.

Work on systems studies for tandem mirror power reactors was largely discontinued in 1986, so there have been few advancements in tandem mirror reactor concepts since that time. If a tandem mirror reactor study were to be done today, it would probably be based on axisymmetric end cells, rather than quadrupole magnets, and take advantage of recent improvement in high energy neutral beams, and free electron lasers and gyrotrons as microwave sources.

The tandem mirror concept has considerable technological advantages as a reactor concept compared with tokamaks, but there remain several critical plasma physics issues which need to be solved experimentally before one can consider building a tandem mirror ignition experiment. These include:

- understanding the loss of plugging in TMX-U,
- achieving reactor relevant parameters in a microstable plasma,
- achieving purely axisymmetric operation with MHD stability,
- developing alternative means of pumping thermal barriers, and
- demonstrating adequate impurity control in a steady-state tandem mirror plasma.

Reasonable next steps in a tandem mirror experimental program would be to:

1. Establish successful operation in an experiment the size of GAMMA-10 but based on axisymmetric end cells and achieve MHD stable operation at a central cell beta of about 25%.
2. Build an experiment of about the size and magnetic field strength of MFTF-B, but with axisymmetric end-cells. Reasonable goals for the central cell parameters would be a density of 3×10^{19} m^{-3}, an ion temperature of 15 keV, an electron temperature of 6 keV, and an $n\tau_p$ of 6×10^{19} m^{-3} s.

Achieving these results would essentially establish the physics basis for proceeding with the tandem mirror as a reactor concept and thereby allow the fusion program to realize the technological advantages of the tandem mirror as a reactor concept.

Acknowledgment

Funding for this work was provided by the Kernforschungszentrum, Karlsruhe, Germany.